Nonlinear dynamics of the solitary wave, boundary-forcing and wave undulation solutions of the nonlinear Equal Width Wave equation

Ali Başhan[1,*]
[1]Bursa Technical University, Faculty of Engineering and Natural Sciences, Dept. of Maths., Bursa, 16310, Türkiye.

e-mail*: alibashan@gmail.com; ali.bashan@btu.edu.tr
Phone*: +90 (224) 808 1232

Abstract

A highly accurate numerical algorithm has been preferred and used to get numerical solutions of solitary wave, boundary-forcing and wave undulation solutions of the nonlinear Equal Width Wave (EW) equation. Since the boundary-forcing solutions of the EW equation do not exist in the literature it's firstly obtained successfully and introduced in this study. Wave generation with different values of the impulse, which is related to the forced-boundary in the EW equation, is investigated. Using low-order modified B-spline and less number of nodal points are two advantages of the present algorithm. Choosing modified cubic B-splines prevents the appearance of the dummy points. To see the difference between the present technique with other methods four applications existing in the literature with many different values of parameters are investigated and comparisons with nearly forty different techniques are reported. For all of the comparisons, undoubtedly present algorithm produces better results except only one method using more than three times nodal points. The produced invariants are also in good agreement with the exact values. Rates of the convergence are computed.

Keywords: Differential quadrature method; Finite difference method; Solitary waves; Equal Width Wave equation; Convergence.

AMS classification: 65N06, 65D32, 74J35, 65M12, 65D07.

1 Introduction

Peregrine [1] first introduced Regularized-long-wave (RLW) equation in 1966 to investigate the development undular bore solutions. The RLW equation is another important equation like the Korteweg-de Vries equation at the applications of non-linear dispersive waves. The RLW equation is of the form

$$u_t + u_x + \varepsilon u u_x - \mu u_{xxt} = 0. \tag{1}$$

Morrison *et al.* [2] suggested the equal width (EW) wave equation of the following form

$$u_t + u u_x - \mu u_{xxt} = 0, \tag{2}$$

where μ is a positive constant.

The nonlinear partial differential equations arise in a wide variety of physical problems such as fluid dynamics, plasma physics, solid mechanics and quantum field theory [3]. In this study, the nonlinear EW equation used in solitary wave modeling will be investigated. Solitary

waves have attracted the interest of researchers due to the diversity of their applications [4]. The EW equation has solitary wave solutions displaying equilibrium between dispersive and nonlinear effects. Analytical and numerical solutions are frequently investigated in the solution of differential equations [5,6]. The exact solutions of the EW equation are limited availability [7–10]. So, many scientist have tried to obtain accurate numerical solutions of the EW equation such as; Gardner and Gardner used Galerkin method [11] based on cubic B-spline, Dağ *et al.* [12] used quadratic B-spline finite element method, Doğan [13] applied linear finite element, Irk [14] used Galerkin method based on Adams-Moulton method, Saka *et al.* [15] applied quartic B-spline based Galerkin method, cosine expansion based differential quadrature method and meshless method, Saka [16] used quadratic Galerkin method with space-splitting technique, space , Haq *et al.* [17] applied collocation method based on septic B- spline, Raslan used collocation method based on quartic B-spline [18], quintic B- spline [19], and finite difference method with contribution of invariant imbedding method [20], Irk *et al.* [21] used collocation method based on cubic B-splines, Saka *et al.* [22] used cubic B-spline collocation method, Dağ and Saka [23] used cubic B-spline collocation method, Dağ and Ersoy [24] used exponential cubic B-spline collocation method, Ghafoor and Haq [25] used Haar wavelet method, Zaki used least-square method [26], and Petrov-Galerkin method [27], Gardner *et al.* [28] used Petrov-Galerkin method with quadratic B-spline function, Roshan [29] used Petrov- Galerkin method with two different order functions, Kaplan and Dereli [30] used radial basis function collocation method, Dereli [31] used augmented radial basis functions collocation method, Banaja and Bakodah [32] used method of lines, Uddin [33] used radial basis function based pseudo-spectral method, Esen and Kutluay [34] used linearized implicit finite-difference method, Esen [35] used lumped Galerkin method, Inan and Bahadır [36] used fully implicit finite difference method, Çelikkaya used operator splitting method [37], Ramos [38] used finite difference methods, Archilla [39] used spectral method, Arora *et al.* [40] used reduced differential transform method, Babolian *et al.* [41] used homotopy analysis method, Yağmurlu and Karakaş [42] used trigonometric cubic B-spline collocation method, Ali [43] used spectral method based on Chebyshev polynomials and Rasoulizadeh et.al. [44] used local meshless method. The novelty of the present study may be given as

- Previously unexplored boundary-forced solutions of the EW equation are obtained.
- By using two numerical methods and contribution of the Rubin-Graves linearizing technique great improvement is observed.
- To see the difference between the present techniques with other classical methods, four applications existing in the literature with many different values of parameters are investigated and comparisons with nearly forty different techniques are reported.

In this study, we aimed to obtain better results than those of earlier routine methods. Main difference of the present study is using two methods together and by means of the addition of advantages caused by two methods obtain successful results. In addition, obtaining boundary-forced solutions of the EW equation, which have not been investigated in previous studies, will be an important contribution to the literature. In order to reduce the workload of the hybrid method, a modified cubic B-spline with diagonal dominant form is preferred. Using low order B-spline as base function also effect the accuracy of the method. Our fundamental technique differential quadrature method (DQM) which has introduced by Bellman *et al.* [45] using less number of mesh points and developed by many applications [45–55]. In this study, just like the Lie Algebra

Approach [56], DQM is used to solve a differential equation whose solution has not been investigated before.

The second section of this paper presents the basic principles of DQM, the third section presents the application of numerical methods to the differential equation, the fourth section presents applications and results, and the last section concludes.

2 The main idea of DQM

Bellman *et al*. [45] suggested a practical and stronger method namely differential quadrature method (in short DQM) based on the integral quadrature idea. The fundamental formulae is below

$$\frac{d^{(r)}f}{dx^{(r)}}(x_i) = \sum_{j=1}^{N} w_{ij}^{(r)} f(x_j), \quad i = 1,2,\dots,N, \; r = 1,2,\dots,N-1 \tag{3}$$

To obtain the weighting coefficients we need the $r-th$ order derivative value of function f. For this purpose, we used as a test function modified cubic B-splines [57]. The advantages of the modification of the cubic B-splines do not create dummy points outside of the solution domain, so we do not need any additional equations. For detailed information on the derivation of modified cubic B-spline functions, see Ref. [57]. From Eq. (3) with value of $r = 1$ and using modified cubic B-splines for the first nodal point x_1 the following equation system is obtained

$$[M]\left[W_1^{(1)}\right] = \left[B_1^{(1)}\right] \tag{4}$$

where

$$[M] = \begin{bmatrix} 6 & 1 & & & & & \\ 0 & 4 & 1 & & & & \\ & 1 & 4 & 1 & & & \\ & & \ddots & \ddots & \ddots & & \\ & & & 1 & 4 & 1 & \\ & & & & 1 & 4 & 0 \\ & & & & & 1 & 6 \end{bmatrix},$$

$$\left[W_1^{(1)}\right] = \left[w_{1,1}^{(1)} \; w_{1,2}^{(1)} \; w_{1,3}^{(1)} \dots \; w_{1,N-1}^{(1)} \; w_{1,N}^{(1)}\right]^T$$

and

$$\left[B_1^{(1)}\right] = [-6/h \;\; 6/h \;\; 0 \dots \;\; 0 \;\; 0]^T.$$

Similarly, for the other nodal points inside the solution domain x_i, $(2 \le i \le N-1)$, respectively,

$$[M]\left[W_i^{(1)}\right] = \left[B_i^{(1)}\right] \tag{5}$$

the following equation system is obtained, where

$$\left[W_i^{(1)}\right] = \left[w_{i,1}^{(1)} \; \dots \; w_{i,i-1}^{(1)} \; w_{i,i}^{(1)} \; w_{i,i+1}^{(1)} \; \dots \; w_{i,N}^{(1)}\right]^T$$

and

$$\left[B_i^{(1)}\right] = [0 \;\dots\; 0 \; -3/h \; 0 \; 3/h \;\; 0 \dots 0]^T.$$

For the last nodal point x_N

$$[M]\left[W_N^{(1)}\right] = \left[B_N^{(1)}\right] \tag{6}$$

the following equation system is obtained, where

$$\left[W_N^{(1)}\right] = \left[w_{N,1}^{(1)} \;\; w_{N,2}^{(1)} \ldots \; w_{N,N-2}^{(1)} \;\; w_{N,N-1}^{(1)} \;\; w_{N,N}^{(1)}\right]^T$$

and

$$\left[B_N^{(1)}\right] = [0 \quad 0 \ldots \; 0 \; -6/h \quad 6/h \quad]^T .$$

Thus, weighting coefficients $w_{i,j}^{(1)}$ which are related to the nodal points $x_i,\ (i = 1,2,\ldots,N)$, are found quite easily by solving the system of Eqs. (4) − (6) with Thomas algorithm. The second order weighting coefficients are obtained by the Shu's recurrence formula [59].

3 Application of the method

We have discretized the EW wave equation (2) given as

$$U_t + UU_x - \mu U_{xxt} = 0.$$

We have implemented the Crank-Nicolson technique. Firstly Eq. (2) is discretized as,

$$\frac{U^{n+1}-U^n}{\Delta t} + \frac{(UU_x)^{n+1}+(UU_x)^n}{2} - \mu\frac{U_{xx}^{n+1}-U_{xx}^n}{\Delta t} = 0 . \tag{7}$$

Eq. (7) is arranged as follows,

$$2U^{n+1} + \Delta t(UU_x)^{n+1} - 2\mu U_{xx}^{n+1} = 2U^n - \Delta t(UU_x)^n - 2\mu U_{xx}^n . \tag{8}$$

Then, Rubin and Graves linearization technique [60] is used to linearize the nonlinear terms and then we have obtained

$$2U^{n+1} + \Delta t(U^{n+1}U_x^n + U^n U_x^{n+1}) - 2\mu U_{xx}^{n+1} = 2U^n - 2\mu U_{xx}^n \ . \tag{9}$$

Now, let us define some terms to be used in Eq. (9) as

$$A_i^n = \sum_{j=1}^N w_{ij}^{(1)} U_j^n = U_{x_i}^n, \quad B_i^n = \sum_{j=1}^N w_{ij}^{(2)} U_j^n = U_{xx_i}^n,$$

$$U_{x_i}^{n+1} = \sum_{j=1}^N w_{ij}^{(1)} U_j^{n+1}, \quad U_{xx_i}^{n+1} = \sum_{j=1}^N w_{ij}^{(2)} U_j^{n+1}, \tag{10}$$

where A_i^n and B_i^n are the 1^{st} and 2^{nd} order derivative approximations of function U at the n^{th} time level on points x_i, respectively. By the substitution of definition (10) in Eq. (9) and reorganizing for each nodal points as follows, we obtain

$$\left[2 + \Delta t\left(A_i^n + U_i^n w_{ii}^{(1)}\right) - 2\mu w_{ii}^{(2)}\right] U_i^{n+1} + \left[\sum_{j=1, i\neq j}^{N} \left(\Delta t U_i^n w_{ij}^{(1)} - 2\mu w_{ij}^{(2)}\right) U_j^{n+1}\right] = P_i^n \tag{11}$$

where

$P_i^n = 2U_i^n - 2\mu B_i^n$, for $i = 1(1)N$.

The matrix form of the equation system is given below

$$\begin{bmatrix} L_{1,1} & L_{1,2} & \dots & L_{1,N} \\ L_{2,1} & L_{2,2} & \dots & L_{2,N} \\ \vdots & \vdots & \ddots & \vdots \\ L_{N-1,1} & L_{N-1,2} & \dots & L_{N-1,N} \\ L_{N,1} & L_{N,2} & \dots & L_{N,N} \end{bmatrix} \begin{bmatrix} U_1^{n+1} \\ U_2^{n+1} \\ \vdots \\ U_{N-1}^{n+1} \\ U_N^{n+1} \end{bmatrix} = \begin{bmatrix} P_1^n \\ P_2^n \\ \vdots \\ P_{N-1}^n \\ P_N^n \end{bmatrix}. \tag{12}$$

Then, the boundary conditions have been applied to the system of Eqs. (12) and for obtaining a solvable system the first and last equations are eliminated. So,

$$\begin{bmatrix} L_{2,2} & L_{2,3} & \dots & L_{2,N-1} \\ L_{3,2} & L_{3,3} & \dots & L_{3,N-1} \\ \vdots & \vdots & \ddots & \vdots \\ L_{N-1,2} & L_{N-1,3} & \dots & L_{N-1,N-1} \end{bmatrix} \begin{bmatrix} U_2^{n+1} \\ U_3^{n+1} \\ \vdots \\ U_{N-1}^{n+1} \end{bmatrix} = \begin{bmatrix} P_2^n - L_{2,1}U_1^{n+1} - L_{2,N}U_N^{n+1} \\ P_3^n - L_{3,1}U_1^{n+1} - L_{3,N}U_N^{n+1} \\ \vdots \\ P_{N-1}^n - L_{N-1,1}U_1^{n+1} - L_{N-1,N}U_N^{n+1} \end{bmatrix} \tag{13}$$

is obtained. The systems can now be solved by Gauss elimination method.

4 Numerical examples, results and comparisons

To check the performance of numerical method the error norms L_2 and L_∞ are used:

$$L_2 = \left(h\sum_{j=1}^{N}\left|u_j - U_j\right|^2\right)^{1/2}, \quad L_\infty = \max_{1\le j\le N}\left|u_j - U_j\right|. \tag{14}$$

The three invariants [61] are calculated as below

$$I_1 = \int_{-\infty}^{\infty} U dx, \quad I_2 = \int_{-\infty}^{\infty}(U^2 + \mu U_x^2)dx, \quad I_3 = \int_{-\infty}^{\infty} U^3 dx, \tag{15}$$

and relative changes of invariants are calculated as below

$$I_p^* = \frac{I_p^{final} - I_p^{initial}}{I_p^{initial}}, \quad p = 1,2,3. \tag{16}$$

The rate of convergence is computed by the formulae as below

$$ROC \cong \frac{\ln\left(Error(N_1)/Error(N_2)\right)}{\ln(N_1/N_2)}.$$

4.1 Motion of the single solitary wave

The analytical solution of single solitary wave is given by Morrison *et.al.* [2]

$$U(x,t) = 3c\,\mathrm{sech}^2[k(x - x_0 - ct)], \tag{17}$$

where $k = \sqrt{\frac{1}{4\mu}}$ is the width of the solitary wave, c is the velocity of the wave and $3c$ is the amplitude of the wave.

The initial condition is obtained from Eq. (17) for the initial time $t = 0$ as below

$$U(x,0) = 3c\,\mathrm{sech}^2[k(x - x_0)], \tag{18}$$

and the boundary conditions are taken as $U(\pm\infty) \to 0$.

The three invariants may be computed analytically as below [28]

$$I_1 = \frac{6c}{k},\ I_2 = \frac{12c^2}{k} + \frac{48kc^2\mu}{5},\ I_3 = \frac{144c^3}{5k}\ .$$

For the extensive survey of the solutions of the single solitary wave, four different velocity values are selected to see the performance of the present method.

Firstly, for the high velocity we use $c = 1.0, \mu = 1, x_0 = 15, \Delta t = 0.05$ and $N = 1571$ at time domain [0, 40] at space interval $0 \le x \le 80$. So, the three invariants obtained analytically by using invariant formulae given by Gardner *et.al.* [28] are $I_1 = 12.0$, $I_2 = 28.8$ and $I_3 = 57.6$. Present numerical results are obtained with fixed parameters. The error norms L_2 and L_∞ and the three invariants are given at Table 1 with other existing results [13, 23, 28, 29, 32]. The fact that the present results are superior of all given results [13,23,28,29,32] may be seen at Table 1. The present invariants I_1, I_2 and I_3 are almost constant and in compliance with analytic results. Relative change of invariants I_1^*, I_2^* and I_3^* at time $t = 40$ are -4.42×10^{-5}, -2.85×10^{-5} and -4.34×10^{-5}, respectively. Motion of the single solitary wave for the velocity $c = 1.0$, during the simulation and maximum error between analytical and numerical results at time $t = 40$ are illustrated at Figure 1. Observation of the Figure 1 shows that the shape, amplitude and velocity of the single solitary wave preserved during the simulation and maximum error at both of the boundaries are zero. This is consistent with the solitary wave theory. The error norms and rate of the convergence related to the space are given at Table 2. By increasing the number of nodal points, the error values decreased and the rates of convergence increased.

Secondly, for the decreasing values of the velocity we use use $c = 0.1, \mu = 1, x_0 = 10, \Delta t = 0.05$ and $N = 261$ at time domain [0, 80] at space interval $0 \le x \le 30$. So, the three invariants are obtained analytically by using invariant formulae given by Gardner et.al. [28] $I_1 = 1.2$, $I_2 = 0.288$ and $I_3 = 0.0576$. The present numerical results are obtained with fixed parameters and very less number of mesh points $N = 261$. Comparison of error norms L_2 and L_∞ and three invariants are given at Table 3. The present results are superior of all given results [12,18,17,21,22,24,25, 28,29,32–37] in the literature at Table 3. The three invariants I_1, I_2 and I_3 remain almost constant and in compliance with analytic results given in Table 3. Relative change of invariants I_1^*, I_2^* and I_3^* at time t = 80 are 2.92×10^{-5}, -1.04×10^{-5} and -1.74×10^{-5}, respectively. Motion of the single solitary wave for the velocity $c = 0.1$, during the simulation and maximum error between analytical and numerical results at time $t = 80$ are illustrated at Figure 2. Observation of the Figure 2 shows that the shape, amplitude and velocity of the single solitary wave are preserved during the simulation. The results obtained reflect the characteristics of solitary waves. The overview of Figure 1 with Figure 2 together shows that by decreasing the amplitudes of the wave the maximum error is decreasing, too. As can be seen from the graphs,

the smaller the amplitude value, the smaller the errors in terms of numerical calculation.

Thirdly, for the decreasing values of the velocity we use $c = 0.03, \mu = 1, x_0 = 10, \Delta t = 0.05$ and $N = 165$ at time domain [0, 80] at space interval $0 \leq x \leq 30$. So, three invariants obtained analytically by using invariant formulae given by Gardner *et.al.* [28] $I_1 = 0.36$, $I_2 = 0.02592$, and $I_3 = 0.001555$. The present numerical results are obtained with fixed parameters and very less number of mesh points $N = 165$. Comparison of error norms L_2 and L_∞ and three invariants are given at Table 4. The present results are superior than the given earlier works [13,17,24,26,29,30,32,34–37] at Table 4. The three lowest invariants I_1, I_2 and I_3 are computed almost constant and in compliance with analytic results given in Table 4. Relative change of invariants I_1^*, I_2^* and I_3^* at time $t = 80$ are 3.33×10^{-5}, 0.00×10^{-6} and 0.00×10^{-6}, respectively. Observation of the Figure 3 shows that the shape, amplitude and velocity of the single solitary wave that has small amplitude preserved during the simulation. Even if the amplitude values were varied, the results exactly reflected the characteristics of solitary waves. The overview of Figure 3 with Figures 1− 2 together shows that by decreasing the amplitudes of the waves the maximum error is decreasing, too.

Fourthly, for the very small value of the velocity we use $c = 0.01, \mu = 1, x_0 = 10, \Delta t = 0.05$ and $N = 190$ over time domain [0, 80] over space interval $0 \leq x \leq 30$. So, three invariants obtained analytically by using invariant formulae given by Gardner *et.al.* [28] $I_1 = 0.12$, $I_2 = 0.00288$, and $I_3 = 0.000058$. The present numerical results are obtained with fixed parameters and very less number of mesh points $N = 190$. The error norms L_2 and L_∞ are given at Table 5. The present error norms are superior of the given earlier works [13, 16, 26, 32, 34, 35] except the error norm L_2 of the Galerkin method [16] at final time of simulation $t = 80$. We must say that the present method used fixed parameters and very less number of mesh points $N = 190$ than all of the earlier works [13, 16, 26, 32, 34, 35] and also Galerkin method [16] N = 600. The three invariants I_1, I_2 and I_3 are almost constant and in compliance with analytic results given in Table 5. Relative change of invariants I_1^*, I_2^* and I_3^* at time $t = 80$ are 0.00×10^{-6}, 0.00×10^{-6} and 0.00×10^{-6}, respectively. Observation of the Figure 4 shows that the shape, amplitude and velocity of the single solitary wave having small amplitude are preserved during the simulation. The overview of Figure 4 with Figures 1− 3 together show that by decreasing the amplitudes of the waves the maximum error is decreasing, too.

4.2 Boundary-forcing

The boundary-forced solution of the EW equation is firstly obtained in the present study. For this application the left boundary condition is chosen as follows

$$U(a,t) = \begin{cases} U_0 \frac{t}{\tau}, & 0 \leq t \leq \tau \\ U_0, & \tau \leq t \leq t_0 - \tau \\ U_0 \frac{t_0 - t}{\tau}, & t_0 - \tau \leq t \leq t_0 \\ 0, & otherwise \end{cases} \tag{19}$$

Here, U_0 is represent the impulse value and τ is represent the period of the impulse which is grows linearly from 0 to U_0. The impulse is effective enough to generate solitary waves at $x = 0$, which grow at a rate determined by the magnitude of the forced boundary value. So, problem is also known as wave maker. The generation of the waves is stopped until the forcing conditions lose. Various values of the impulse U_0 is chosen to observe the behavior of the waves

clearly. The period is fixed as $\tau = 0.1$ with total period of $t_0 = 30$ for all applications. All of the applications are simulated over the region $0 \leq x \leq 300$ with $\Delta t = 0.1$ and $h = 0.1$.

Firstly, a small value of impulse $U_0 = 1$ is chosen. At the time close to $t = 50$ two great waves and behind them one small wave is occurred. At the end of the simulation, the generated waves are seen clearly. Simulations of the first application is given in Figure 5.

Secondly, a greater impulse value is chosen as $U_0 = 2$. The simulations plotted and given in Figure 6. The waves occur step by step and five different waves are occurred at the time close to $t = 50$. At the end of the simulation five separated waves are seen clearly.

Lastly, the greatest impulse value is chosen as $U_0 = 3$. The simulations are plotted and given in Figure 7. The generation of the waves continue until to time $t = 50$. Seven different waves are generated.

The three invariants are computed for all applications and reported in Table 6. The invariant values are observed almost constant after the time $t = 50$. This means that generation of the waves are finished. The graph of the development of the conserved quantities is given in Figure 8.

4.3 The wave undulation

The wave undulation has the initial condition [28] as follow

$$U(x,0) = \frac{U_0}{2}\left[1 - \tanh\left(\frac{x-x_c}{d}\right)\right].$$

The height of the water level from equilibrium is represented by $U(x,0)$ and x_c denotes the center of the magnitude U_0. The steepness of the change is measured by d. The left boundary condition is given as $U \to U_0$ when $x \to -\infty$ and $U \to 0$ when $x \to \infty$. The conservation quantities are increased linearly and their rates can be calculated as [28]

$$M_1 = \frac{d}{dt} I_1 = \frac{d}{dt}\int_{-\infty}^{\infty} u dx = 0.5(U_0)^2,$$

$$M_2 = \frac{d}{dt} I_2 = \frac{d}{dt}\int_{-\infty}^{\infty} (u^2 + \mu(u_x)^2) dx = \frac{2(U_0)^3}{3},$$

$$M_3 = \frac{d}{dt} I_3 = \frac{d}{dt}\int_{-\infty}^{\infty} u^3 dx = \frac{3(U_0)^4}{4}.$$

The chosen constant parameters are $\mu = 1/6$, $U_0 = 0.1$, the computed results are obtained as $M_1 = 0.005000$, $M_2 = 0.000667$, $M_3 = 0.000075$. The growth rates for invariants are calculated numerically by the following formulae

$$M_j = \frac{I_j^{final} - I_j^{initial}}{Total\ time}, \quad j = 1,2,3. \tag{20}$$

Numerical simulations are obtained over the domain $-20 \leq x \leq 50$ for various values of the steepness $d = 1, d = 2, d = 5, d = 10$. The numerical values are obtained from formulae (20) for $d = 1$ as $M_1 = 0.00499998$, $M_2 = 0.00066678$, $M_3 = 0.0000750425$. Numerical results are in good agreements with analytical ones. Numerical results for all of the values of the steepness are collected and given in Table 7. The three invariants, their locations and the amplitudes have small

differences. To be able to observe the effect of the steepness the graphs are given separately in Figures 9−12.

When steepness value is increased the undulation of the wave decreased and by the decreasing of the steepness value the propagation of the waves are getting faster.

5 Conclusion

The equal width wave equation has been solved numerically with high accuracy by using very less number of mesh points. Solitary wave, boundary-forcing and wave undulation solutions of the nonlinear EW equation obtained successfully. The boundary-forcing solutions of the EW equation is firstly obtained and introduced in the present study. Two efficient numerical methods are used together and better results are obtained by using the same parameters with earlier methods in the literature. To observe the behaviour of the waves, all test problems for all different values of parameters are illustrated with details. This stronger joined method may be useful for the studies planned in the future. On the other hand, in this study, solutions of equations with a single nonlinear term are investigated. The effectiveness of the method for more complex problems can be tested in future studies.

References

[1] Peregrine, D.H. ”Calculations of the development of an undular bore”, *J. Fluid Mech.*, **25**, part 2, pp. 321-330 (1966). https://doi.org/10.1017/S0022112066001678

[2] Morrison, P.J. , Meiss, J.D. and Cary, J.R. ”Scattering of Regularized-Long-Wave solitary waves”, *Physica 11D*, 324-336 (1984). https://doi.org/10.1016/0167-2789(84)90014-9

[3] Wazwaz, A-M. ”Partial Differential Equations and Solitary Waves Theory”, Higher Education Press, *Beijing and Springer-Verlag Berlin Heidelberg* (2009).

[4] Yasin, F., Alshehri, M.H., Arshad, M., et al. ”Exploring dynamics of multi-peak and breathers-type solitary wave solutions in generalized higher-order nonlinear Schrödinger equation and their optical applications”, *Alexandria Engineering Journal* **105**, 402-413 (2024). https://doi.org/10.1016/j.aej.2024.07.082

[5] Wang, B., Kharazian, E. and Grolet, A. ”Application of Normal Form Theory to Power Systems: A Proof of Concept of a Novel Structure-Preserving Approach”, 2024 IEEE Power Energy Society General Meeting (PESGM) | *USGov* |https://doi.org/10.1109/PESGM51994.2024.10688514

[6] Jafarzadeh, E., Kabiri-Samani, A., Boroomand, B., et al. ”Analytical modeling of flexible circular submerged mound motion in gravity waves”, *Journal of Ocean Engineering and Marine Energy*, **9**, 181-190 (2023). https://doi.org/10.1007/s40722-022-00248-9

[7] Biazar, J. and Ayati, Z. ”Application of the Exp-function method to the equal width wave equation”, *Phys. Scr*. **78**, 045005 (4pp) (2008). https://doi.org/10.1088/0031-8949/78/04/045005

[8] Ali, H.A., Biswas, A. and Raslan, K.R. ”Application of Hes Exp-function method and semi

inverse variational principle to equal width wave (EW) and modified equal width wave (MEW)", *International Journal of the Physical Sciences*, **7**(7), 1035-1043 (2012). DOI: 10.5897/IJPS11.1755

[9] Lu, D., Seadawy, A.R. and Ali, A. "Dispersive traveling wave solutions of the Equal-Width and Modified Equal-Width equations via mathematical methods and its applications", *Results in Physics*, **9**, 313–320 (2018). https://doi.org/10.1016/j.rinp.2018.02.036

[10] Nuruddeen, R.I., Aboodh, K.S. and Ali, K.K. "Investigating the tangent dispersive solitary wave solutions to the Equal Width and Regularized Long Wave equations", *Journal of King Saud University and Science*, **32**, 677-681 (2020). https://doi.org/10.1016/j.jksus.2018.10.016

[11] Gardner, L.R.T. and Gardner, G.A. "Solitary waves of the equal width wave equation", *J Comput.Phys.*, **101**, 218-223 (1992). https://doi.org/10.1016/0021-9991(92)90054-3

[12] Dağ, I., Irk, D. and Boz, A. "Simulation of EW Wave Generation via Quadratic B-spline Finite Element Method", *International Journal of Mathematics and Statistics*, **1**(A07) 46-59 (2007).

[13] Doğan, A. "Application of Galerkin's method to equal width wave equation", *Applied Mathematics and Computation*, **160**, 65–76 (2005). https://doi.org/10.1016/j.amc.2003.08.105

[14] Irk, D. "B-Spline Galerkin Solutions for the Equal Width Equation", *Physics of Wave Phenomena*, **20**(2), 122–130 (2012). https://doi.org/10.3103/S1541308X12020057

[15] Saka, B., Dağ, I., Dereli, Y. et al. "Three different methods for numerical solution of the EW equation", *Engineering Analysis with Boundary Elements*, **32**, 556–566 (2008). https://doi.org/10.1016/j.enganabound.2007.11.002

[16] Saka, B. "A finite element method for equal width equation", *Applied Mathematics and Computation*, **175**, 730–747 (2006). https://doi.org/10.1016/j.amc.2005.07.034

[17] Haq, F., Shah, I.A., and Ahmad, S. "Septic B-Spline Collocation method for numerical solution of the Equal Width Wave (EW) equation", *Life Science Journal*, **10**(1s), 253-260 (2013).

[18] Raslan, K.R. "Collocation method using quartic B-spline for the equal width (EW) equation", *Applied Mathematics and Computation*, **168**, 795–805 (2005). https://doi.org/10.1016/j.amc.2004.09.019

[19] Raslan, K.R. "A computational method for the equal width equation", *International Journal of Computer Mathematics*, **81**(1), 63–72 (2004). https://doi.org/10.1080/00207160310001614963

[20] Raslan, K.R. "Numerical methods for partial differential equations", PhD thesis, Al-Azhar University, Cairo (1999).

[21] Irk, D., Saka, B. and Dağ, I. "Cubic spline collocation method for the equal width equation", *Hadronic Journal Supplement*, **18**, 201-214 (2003).

[22] Saka, B., Irk, D. and Dağ, I. "A Numerical study of the equal width equation", *Hadronic Journal Supplement*, **18**, 99-116 (2003).

[23] Dağ, I. and Saka, B. ”A Cubic B-Spline Collocation Method for the EW Equation”, *Mathematical and Computational Applications*, **9**(3), 381-392 (2004). https://doi.org/10.3390/mca9030381

[24] Dağ, I. and Ersoy, O. ”The exponential cubic B-spline algorithm for equal width equation”, *Advanced Studies in Contemporary Mathematics*, **25**(4) 525-535 (2015).

[25] Ghafoor, A. and Haq, S. ”An efficient numerical scheme for the study of equal width equation, *Results in Physics*, **9**, 1411-1416 (2018). https://doi.org/10.1016/j.rinp.2018.04.060

[26] Zaki, S.I. ”A least-squares finite element scheme for the EW equation”, *Comput. Methods Appl. Mech. Engrg.*, **189**, 587-594 (2000). https://doi.org/10.1016/S0045-7825(99)00312-6

[27] Zaki, S.I. ”Solitary waves induced by the boundary forced EW equation”, *Comput. Methods Appl. Mech. Engrg.*, **190**, 4881-4887 (2001). https://doi.org/10.1016/S0045-7825(99)00462-4

[28] Gardner, L.R.T., Gardner, G.A., Ayoub, F.A., et al. ”Simulations of the EW undular bore”, *Communications in Numerical Methods in Engineering*, **13**, 583-592 (1997). https://doi.org/10.1002/(SICI)1099-0887(199707)13:7<583::AID-CNM90>3.0.CO;2-E

[29] Roshan, T. ”A Petrov–Galerkin method for equal width equation”, *Applied Mathematics and Computation*, **218**, 2730–2739 (2011). https://doi.org/10.1016/j.amc.2011.08.013

[30] Kaplan, A.G. and Dereli, Y. ”Numerical Solution of the EW Equation with Radial Basis Function Collocation Method”, *Suleyman Demirel Universitesi, Fen Bilimleri Enstitusu dergisi*, **16**(1), 48-55 (2012).

[31] Dereli, Y. ”Numerical Solution of the Equal Width Equation Using Augmented Radial Basis Functions Collocation Method”, *Selcuk Journal of Applied Mathematics*, **15**(2), 1-17 (2014).

[32] Banaja, M.A. and Bakodah, H.O. ”Runge-Kutta Integration of the Equal Width Wave Equation Using the Method of Lines”, *Mathematical Problems in Engineering*, Volume **2015**, Article ID 274579, 9 pages http://dx.doi.org/10.1155/2015/274579

[33] Uddin, M. ”RBF-PS scheme for solving the equal width equation”, *Applied Mathematics and Computation*, **222**, 619–631 (2013). http://dx.doi.org/10.1016/j.amc.2013.07.031

[34] Esen, A. and Kutluay, S. ”A linearized implicit finite-difference method for solving the equal width wave equation”, *International Journal of Computer Mathematics*, **83**(3), 319–330 (2006). https://doi.org/10.1080/00207160600740958

[35] Esen, A. ”A numerical solution of the equal width wave equation by a lumped Galerkin method”, *Applied Mathematics and Computation*, **168**, 270–282 (2005). https://doi.org/10.1016/j.amc.2004.08.013

[36] İnan, B. and Bahadır, A.R. ”A numerical solution of the equal width wave equation using a fully implicit finite difference method”, *Turkish Journal of Mathematics and Computer Science*, (2014), Article ID 20140037, 1-14

[37] Çelikkaya, ˙ I. ”Operator Splitting Solution of Equal Width Wave Equation Based on the Lie-Trotter and Strang Splitting Methods”, *Konuralp Journal of Mathematics*, **6**(2), 200-208

(2018).

[38] Ramos, J.I. ”Solitary waves of the EW and RLW equations”, *Chaos, Solitons and Fractals*, **34**, 1498–1518 (2007). https://doi.org/10.1016/j.chaos.2006.04.015

[39] Archilla, B.G. ”A Spectral Method for the Equal Width Equation”, *Journal of Computational Physics*, **125**, 395–402 (1996). https://doi.org/10.1006/jcph.1996.0101

[40] Arora, R., Siddiqui, M.J. and Singh, V.P. ”Solutions of Inviscid Burgers’ and Equal Width Wave Equations by RDTM”, *International Journal of Applied Physics and Mathematics*, **2**(3), May 2012 https://www.ijapm.org/show-31-136-1.html#:~:text=DOI%3A%2010.7763/IJAPM.2012.V2.92

[41] Babolian, E., Saeidian, J. and Paripour, M. ”Application of the Homotopy Analysis Method for Solving Equal-Width Wave and Modified Equal-Width Wave Equations”, *Z. Naturforsch*, **64a**, 685 – 690 (2009). https://doi.org/10.1515/zna-2009-1103

[42] Yağmurlu, N.M. and Karakaş, A.S. ”Numerical solutions of the equal width equation by trigonometric cubic B-spline collocation method based on Rubin-Graves type linearization”, *Numer Methods Partial Differential Eq.*, **36**, 1170-1183 (2020). https://doi.org/10.1002/num.22470

[43] Ali, A.H.A. ”Spectral method for solving the equal width equation based on Chebyshev polynomials”, *Nonlinear Dyn.*, **51** 59–70 (2008). https://doi.org/10.1007/s11071-006-9191-0

[44] Rasoulizadeh, M.N., Ebadi, M.J., Avazzadeh, Z. et al. ”An efficient local meshless method for the equal width equation in fluid mechanics”, *Engineering Analysis with Boundary Elements*, **131** 258-268 (2021). https://doi.org/10.1016/j.enganabound.2021.07.001

[45] Bellman, R., Kashef, B.G. and Casti, J. ”Differential quadrature: a technique for the rapid solution of nonlinear differential equations”, *Journal of Computational Physics*, **10**, 40-52 (1972). https://doi.org/10.1016/0021-9991(72)90089-7

[46] Başhan, A. ”Numerical dynamics of the Generalized Equal Width (GEW) wave equation in presence of high-order nonlinearity”, *Indian J Pure Appl Math.*, **55**, 1365-1388 (2024). https://doi.org/10.1007/s13226-023-00444-9

[47] Başhan, A. ”A novel outlook to the an alternative equation for modelling shallow water wave: Regularised Long Wave (RLW) equation”, *Indian J Pure Appl Math.*, **54**, 133-145 (2023). https://doi.org/10.1007/s13226-022-00239-4

[48] Başhan, A. ”Solitary wave, undular-bore and wave-maker solutions of the cubic, quartic and quintic nonlinear generalized equal width (GEW) wave equation”, *Eur. Phys. J. Plus* (2023). **138**:53 https://doi.org/10.1140/epjp/s13360-023-03648-4

[49] Başhan, A. ”A novel outlook to the mKdV equation using the advantages of a mixed method”, *Applicable Analysis*, **102**(1), 65-87 (2023). https://doi.org/10.1080/00036811.2021.1947493

[50] Başhan, A., Uçar, Y., Yağmurlu, N.M., et al. ”Numerical approximation to the MEW

equation for the single solitary wave and different types of interactions of the solitary waves", *Journal of Difference Equations and Applications*, **28**:9, 1193-1213, (2022). https://doi.org/10.1080/10236198.2022.2132154

[51] Başhan, A. "Nonlinear dynamics of the Burgers equation and numerical experiments", *Mathematical Sciences*, **16**, 183-205 (2022). https://doi.org/10.1007/s40096-021-00410-8

[52] Başhan, A. and Yağmurlu, N.M. "A mixed method approach to the solitary wave, undular bore and boundary-forced solutions of the Regularized Long Wave equation", *Computational and Applied Mathematics*, **41**(169), (2022). https://doi.org/10.1007/s40314-022-01882-7

[53] Başhan, A. "Bell-shaped soliton solutions and travelling wave solutions of the fifth-order nonlinear modified Kawahara equation", *IJNSNS*, **22**(6), 781-795 (2021). https://doi.org/10.1515/ijnsns-2019-0071

[54] Başhan, A., Yağmurlu, N.M., Uçar, Y., et al. "A new perspective for the numerical solution of the Modified Equal Width wave equation", *Math Meth Appl Sci*., **44**, 8925-8939. (2021). https://doi.org/10.1002/mma.7322

[55] Başhan, A. "Modification of quintic B-spline differential quadrature method to nonlinear Korteweg-de Vries equation and numerical experiments", *Applied Numerical Mathematics*, **167**, 356-374 (2021). https://doi.org/10.1016/j.apnum.2021.05.015

[56] Shang, Y. "A Lie algebra approach to susceptible-infected-susceptible epidemics", *Electronic Journal of Differential Equations*, **2012**(233), pp. 1-7. (2012). URL: http://ejde.math.txstate.edu

[57] Mittal, R.C. and Jain, R.K. "Numerical solutions of Nonlinear Burgers' equation with modified cubic B-splines collocation method", *Appl. Math. Comp*., **218**, 7839-7855 (2012). https://doi.org/10.1016/j.amc.2012.01.059

[58] Prenter, P.M. "Splines and Variational Methods", *John Wiley, New York*, (1975).

[59] Shu, C. "Differential Quadrature and its application in engineering", *Springer-Verlag London Ltd.* (2000).

[60] Rubin S.G. and Graves, R.A. "A cubic spline approximation for problems in fluid mechanics", National aeronautics and space administration, Technical Report, Washington, (1975).

[61] Olver, P.J. "Euler operators and conservation laws of the BBM equation", *Math Proc. Camb. Phil. Soc*., **85**, 143-160 (1979). https://doi.org/10.1017/S0305004100055572

Figure and Table captions

Figure 1: Motion of single solitary wave and maximum error: $c = 1.0$

Figure 2: Motion of single solitary wave and maximum error: $c = 0.1$

Figure 3: Motion of single solitary wave and maximum error: $c = 0.03$

Figure 4: Motion of single solitary wave and maximum error: $c = 0.01$

Figure 5: The boundary-forcing: $U_0 = 1$

Figure 6: The boundary-forcing: $U_0 = 2$

Figure 7: The boundary-forcing: $U_0 = 3$

Figure 8: The invariants for boundary-forcing: $U_0 = 1, U_0 = 2, U_0 = 3$

Figure 9: The wave undulation: $d = 1$

Figure 10: The wave undulation: $d = 2$

Figure 11: The wave undulation: $d = 5$

Figure 12: The wave undulation: $d = 10$

Table 1: Single solitary wave: $c = 1.0, \mu = 1, 0 \leq x \leq 80$.

Table 2: Error norms and rates of convergence at $t = 40 : c = 1.0, \mu = 1,\ 0 \leq x \leq 80$.

Table 3: Single solitary wave: $c = 0.1, \mu = 1,\ 0 \leq x \leq 30$.

Table 4: Single solitary wave: $c = 0.03, \mu = 1,\ 0 \leq x \leq 30$.

Table 5: Single solitary wave: $c = 0.01, \mu = 1,\ 0 \leq x \leq 30$.

Table 6: The three invariants for boundary-forcing: $U_0 = 1, U_0 = 2, U_0 = 3$

Table 7: The three invariants, location and amplitude of the leading undulation: $\Delta t = 0.2$, $h = 0.2$.

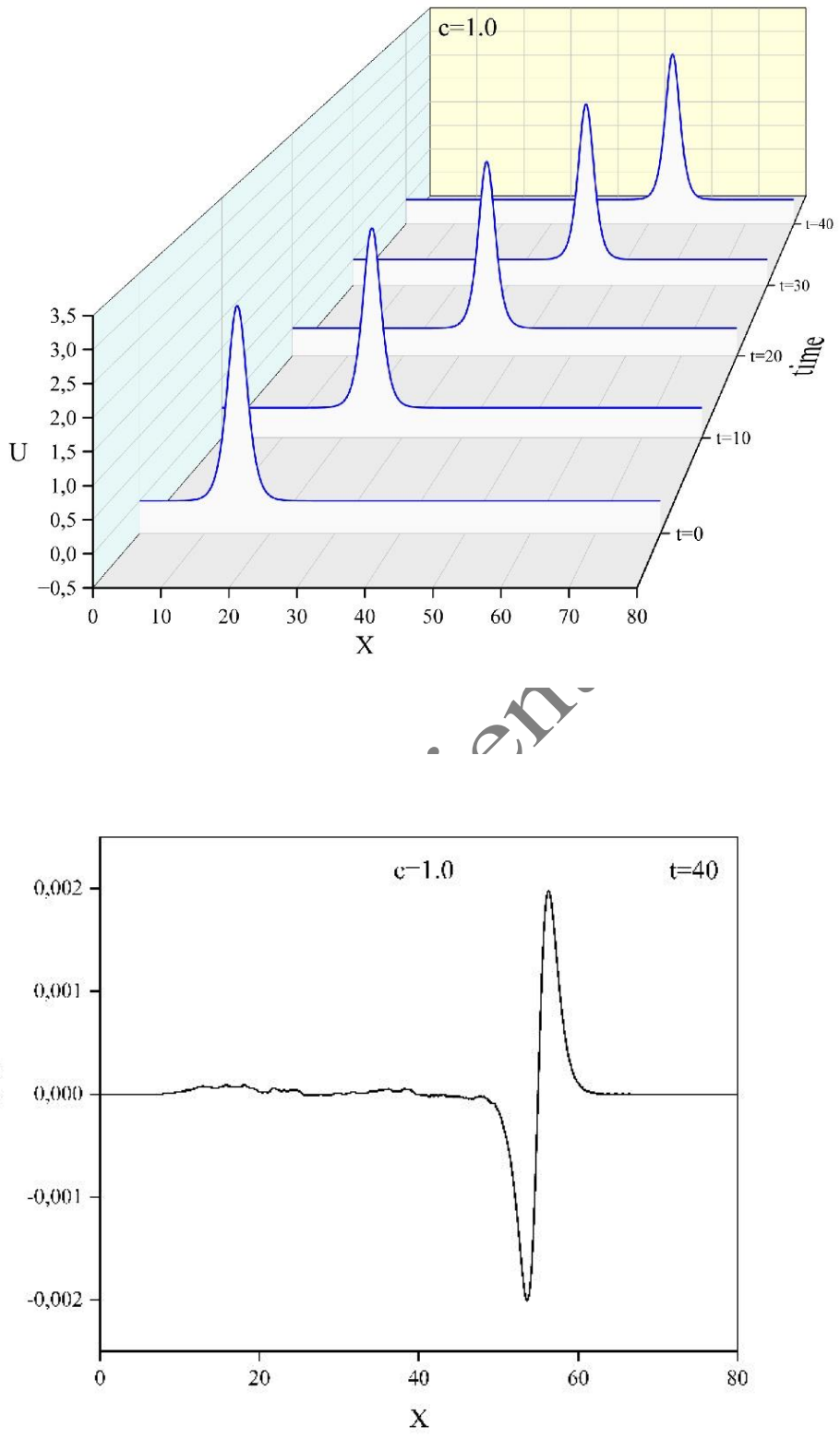

Figure 1: Motion of single solitary wave and maximum error: $c = 1.0$

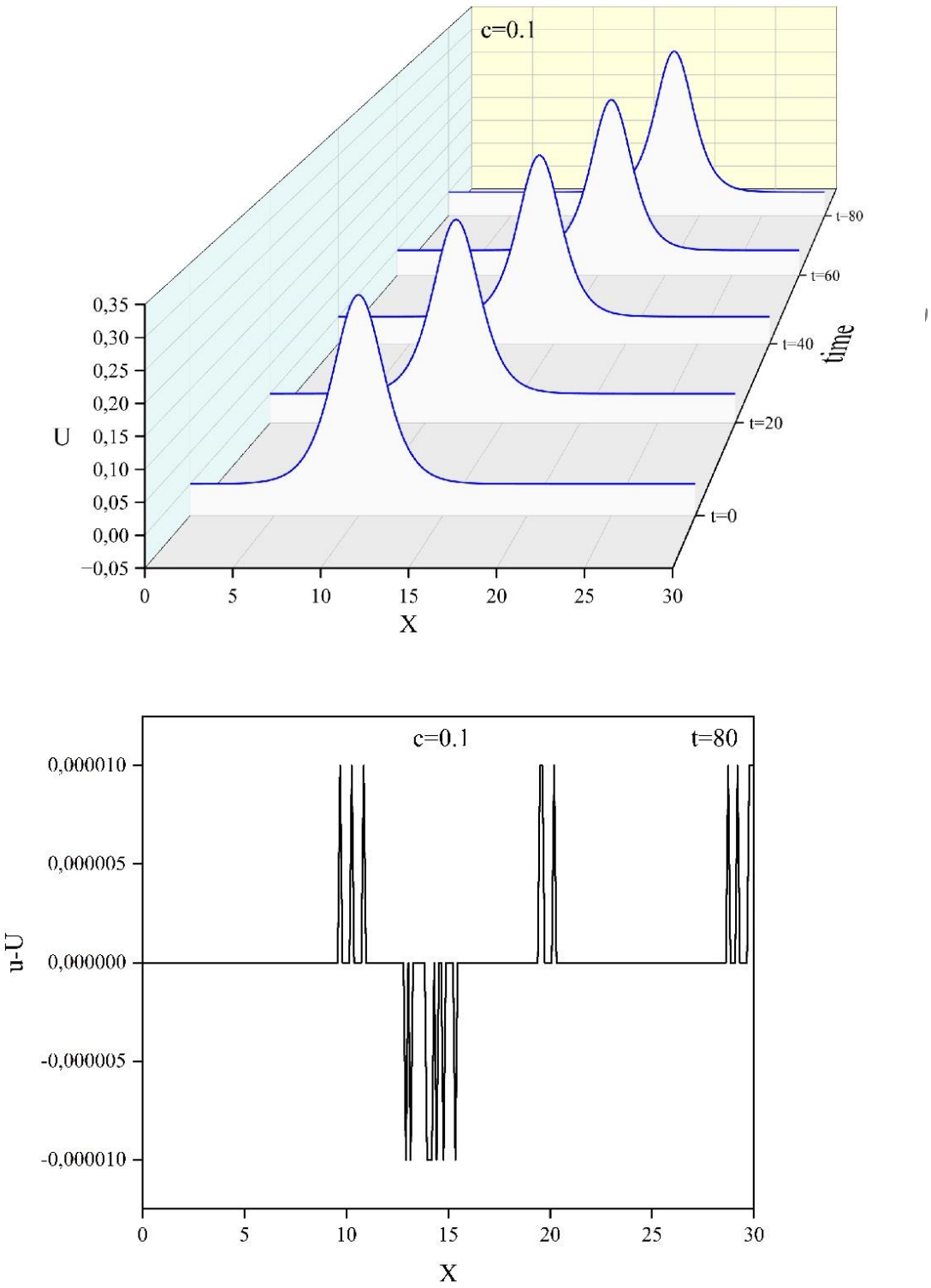

Figure 2: Motion of single solitary wave and maximum error: $c = 0.1$

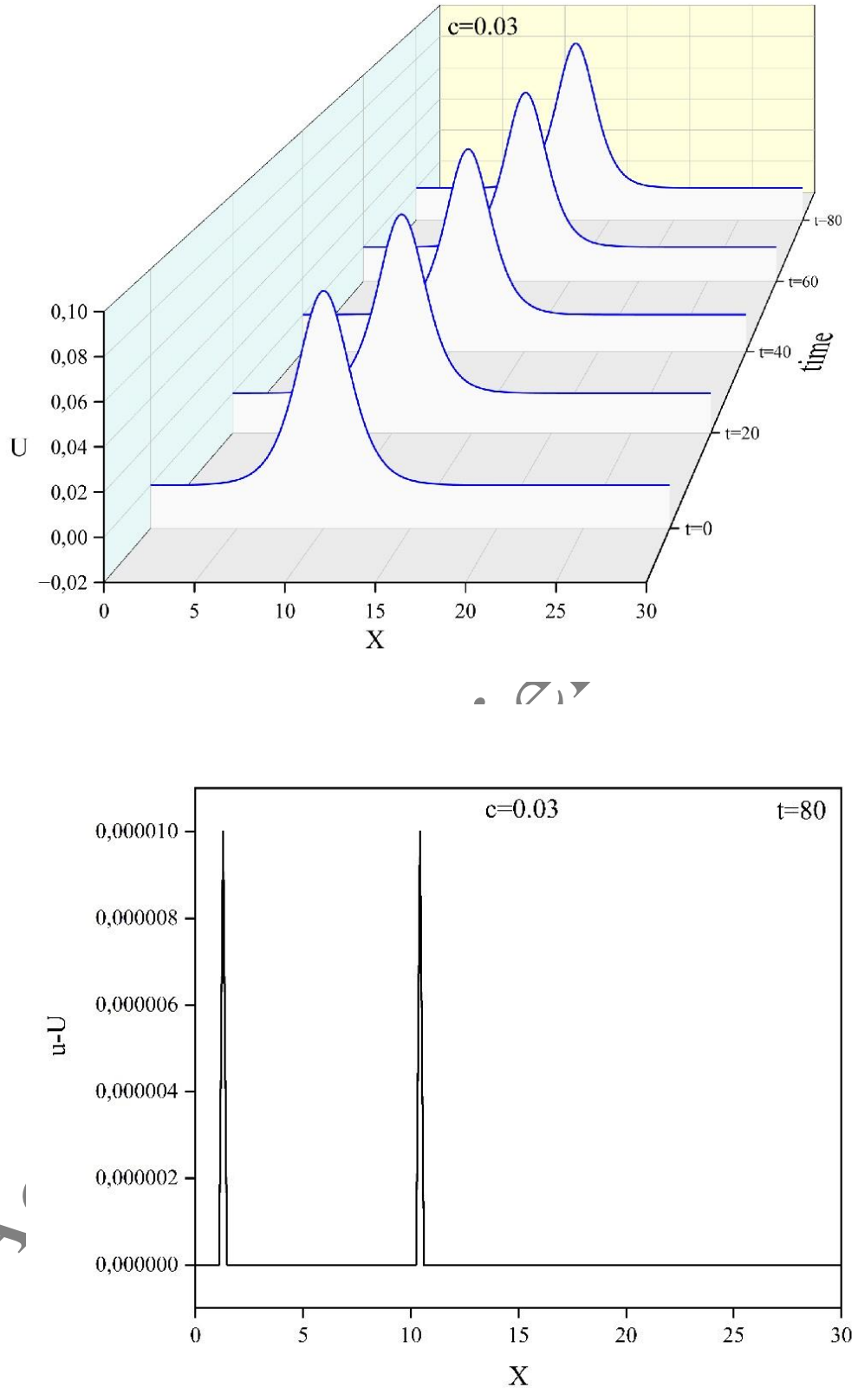

Figure 3: Motion of single solitary wave and maximum error: $c = 0.03$

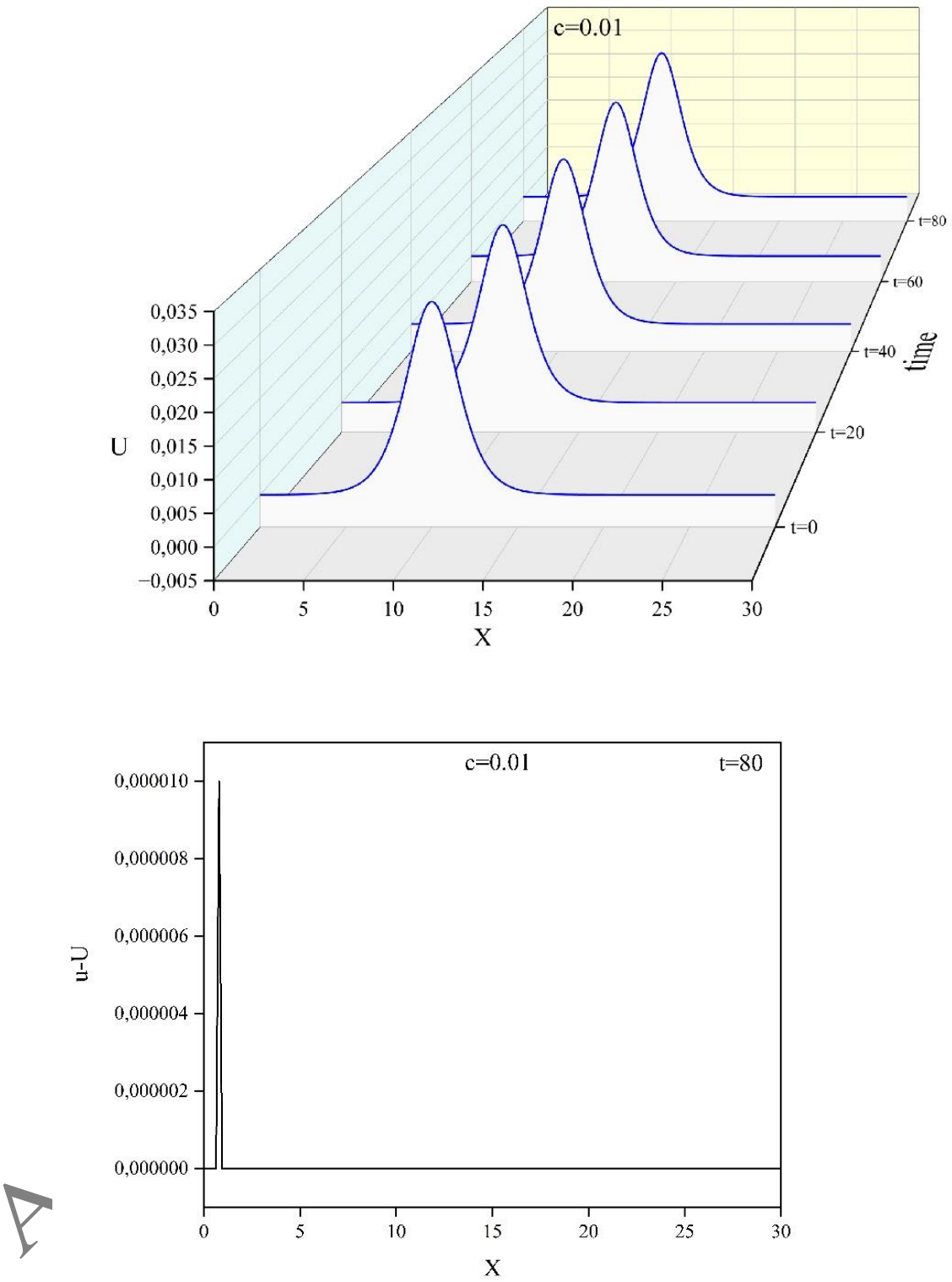

Figure 4: Motion of single solitary wave and maximum error: $c = 0.01$

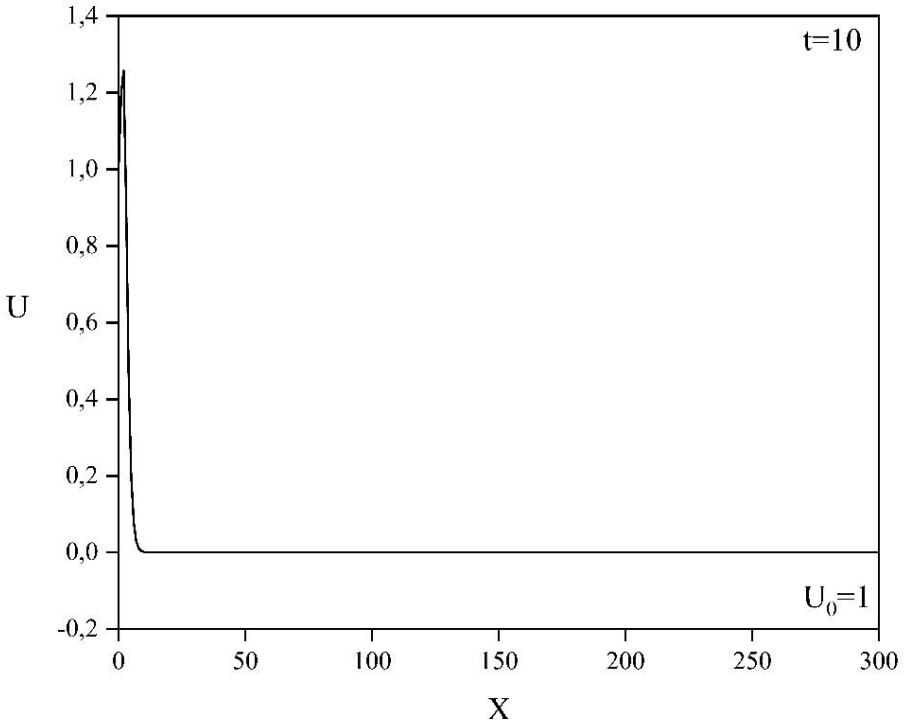
t=10
U
X
U_0=1
1,4
1,2
1,0
0,8
0,6
0,4
0,2
0,0
-0,2
0
50
100
150
200
250
300

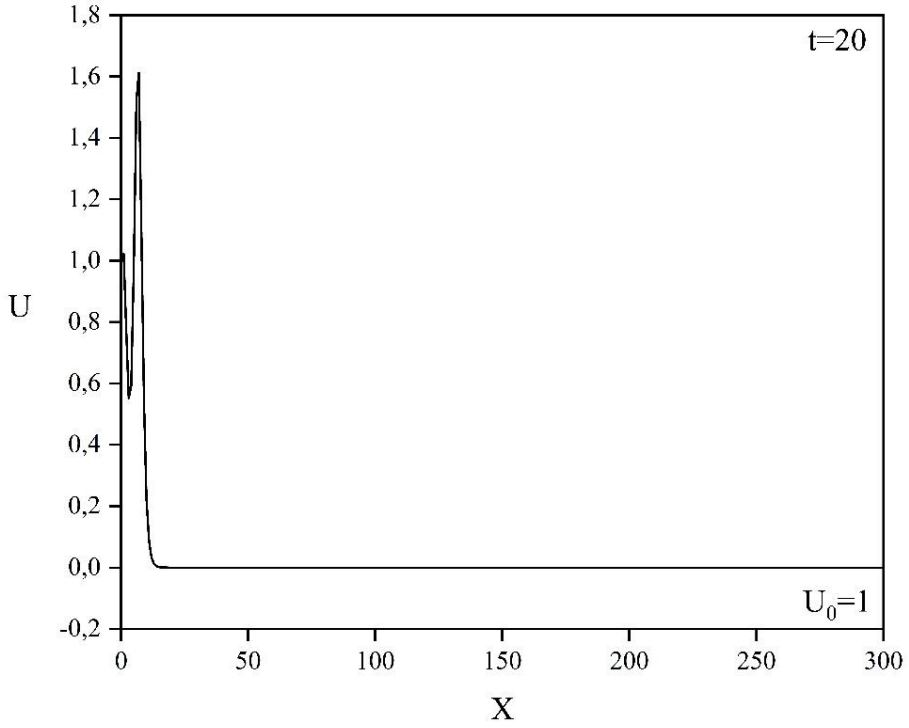
t=20
U
X
U_0=1
1,8
1,6
1,4
1,2
1,0
0,8
0,6
0,4
0,2
0,0
-0,2
0
50
100
150
200
250
300

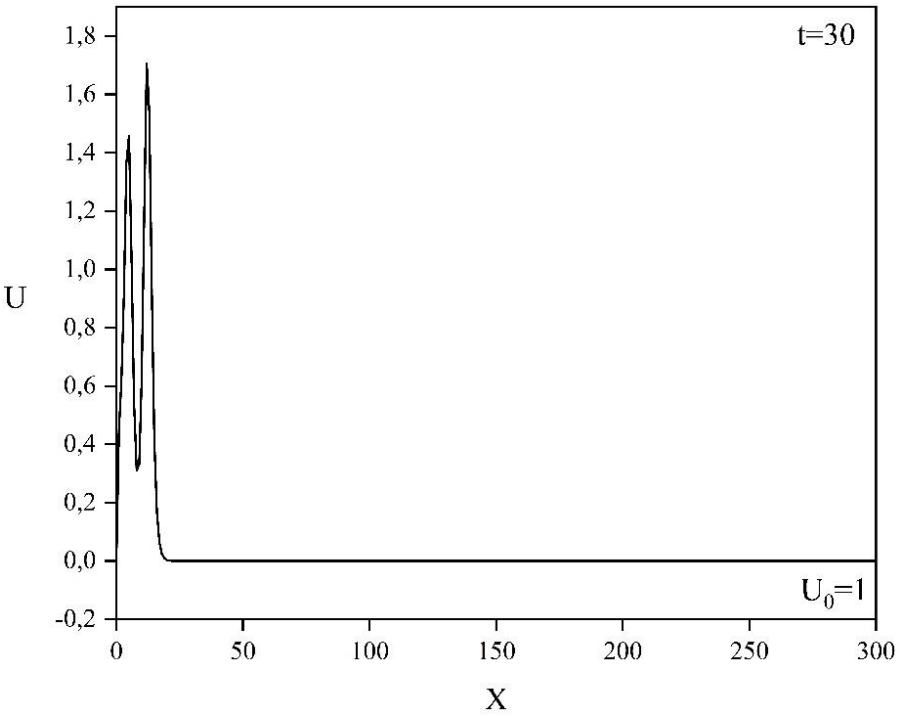
t=30
U
X
U_0=1
1,8
1,6
1,4
1,2
1,0
0,8
0,6
0,4
0,2
0,0
-0,2
0
50
100
150
200
250
300

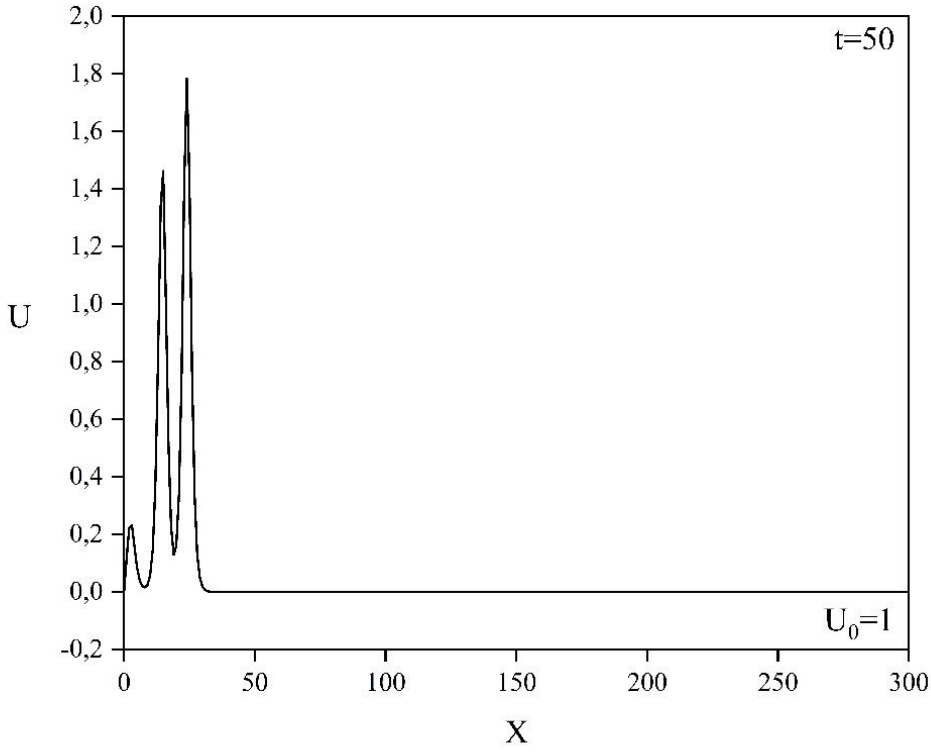
t=50
U
X
U_0=1
2,0
1,8
1,6
1,4
1,2
1,0
0,8
0,6
0,4
0,2
0,0
-0,2
0
50
100
150
200
250
300

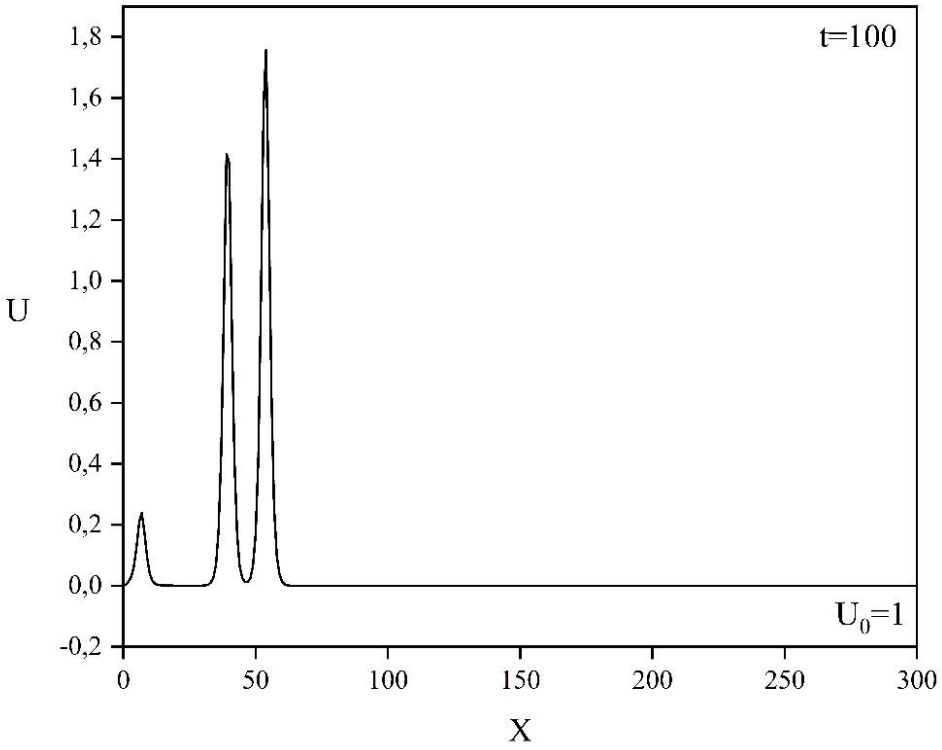

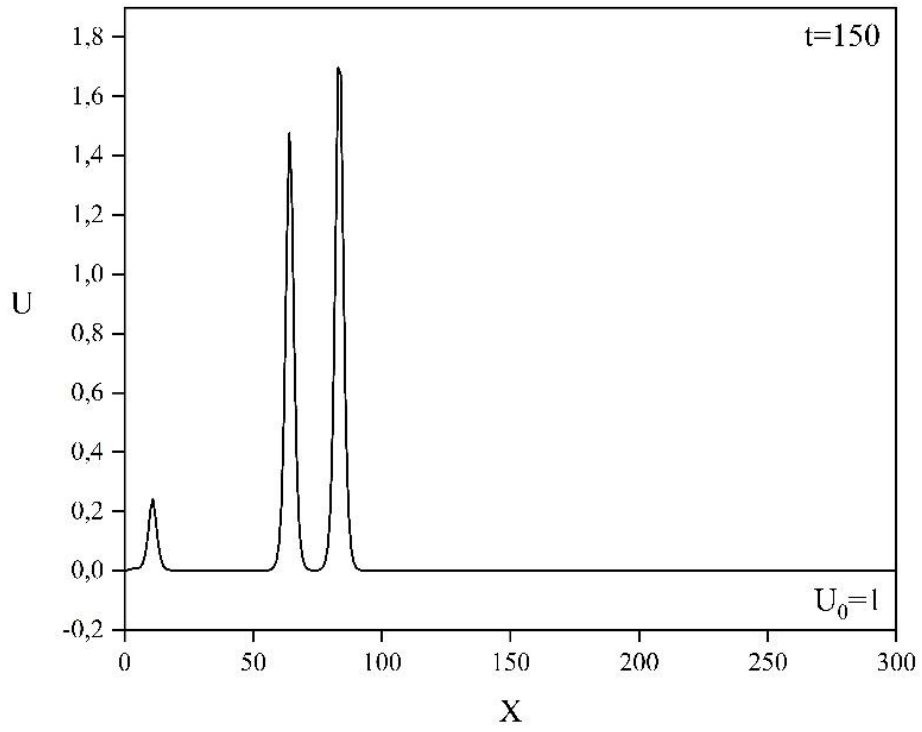

Figure 5: The boundary-forcing: $U_0 = 1$

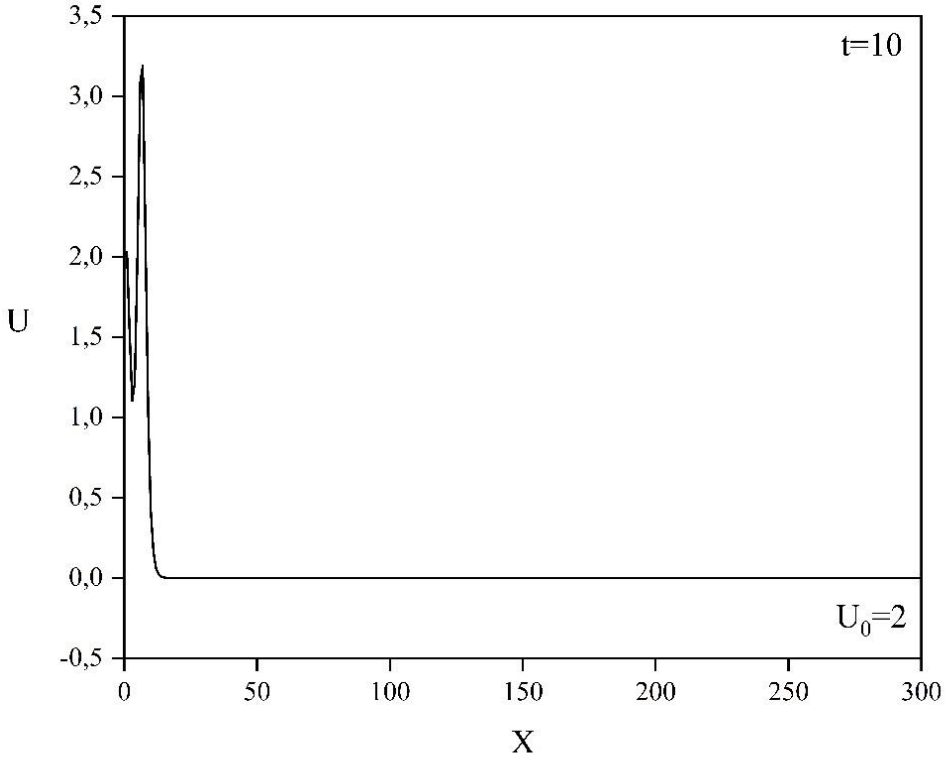
t=10
U
X
U_0=2
3,5
3,0
2,5
2,0
1,5
1,0
0,5
0,0
-0,5
0
50
100
150
200
250
300

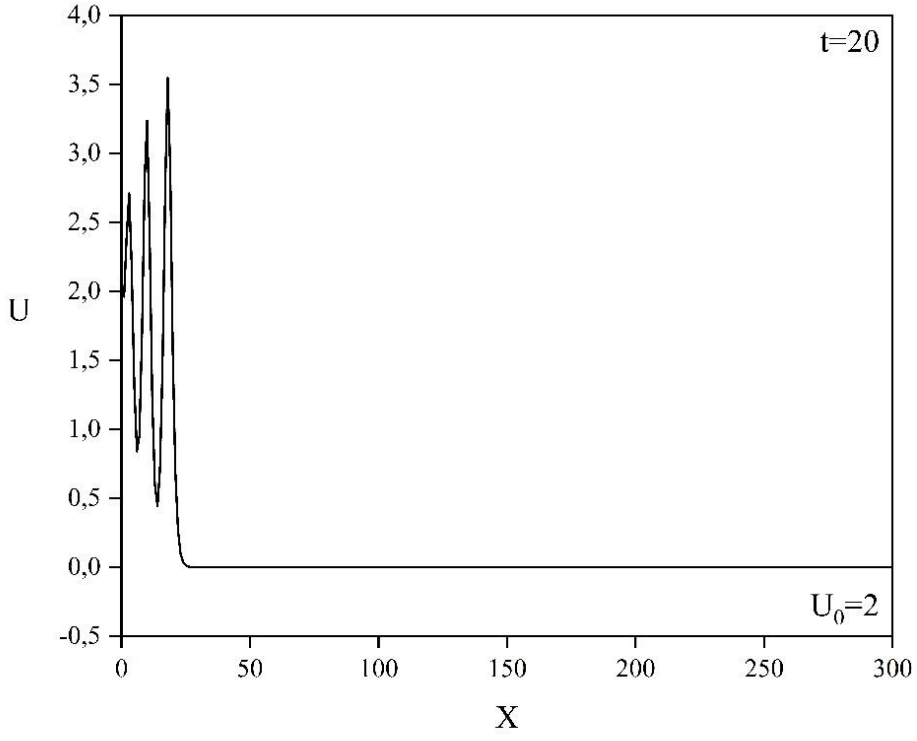
t=20
U
X
U_0=2
4,0
3,5
3,0
2,5
2,0
1,5
1,0
0,5
0,0
-0,5
0
50
100
150
200
250
300

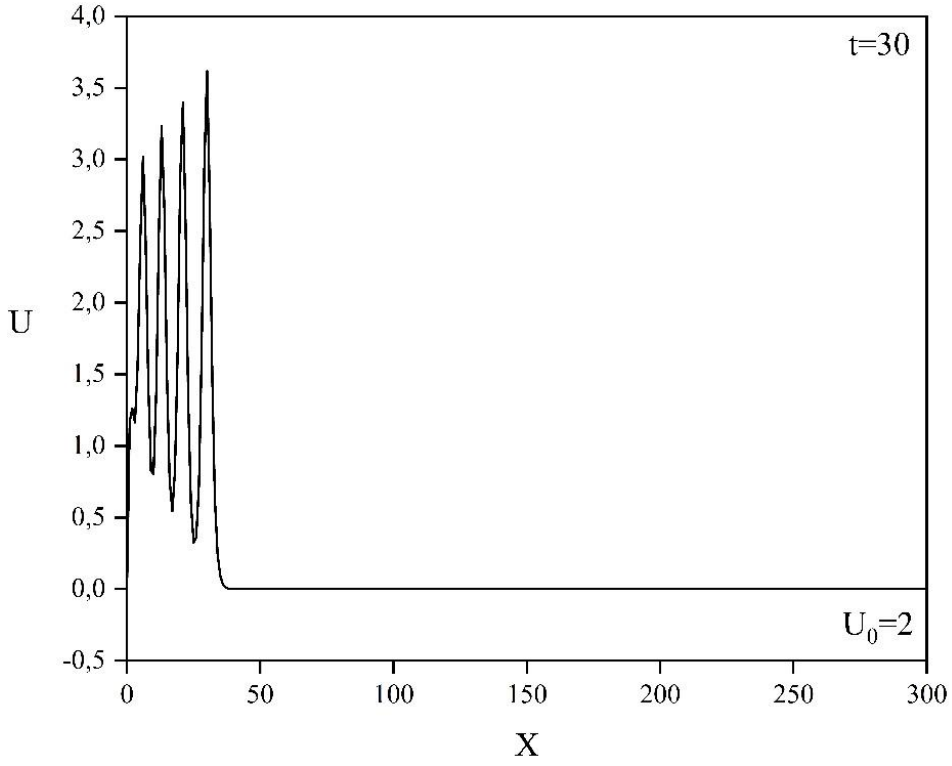
t=30
U
X
U_0=2
4,0
3,5
3,0
2,5
2,0
1,5
1,0
0,5
0,0
-0,5
0
50
100
150
200
250
300

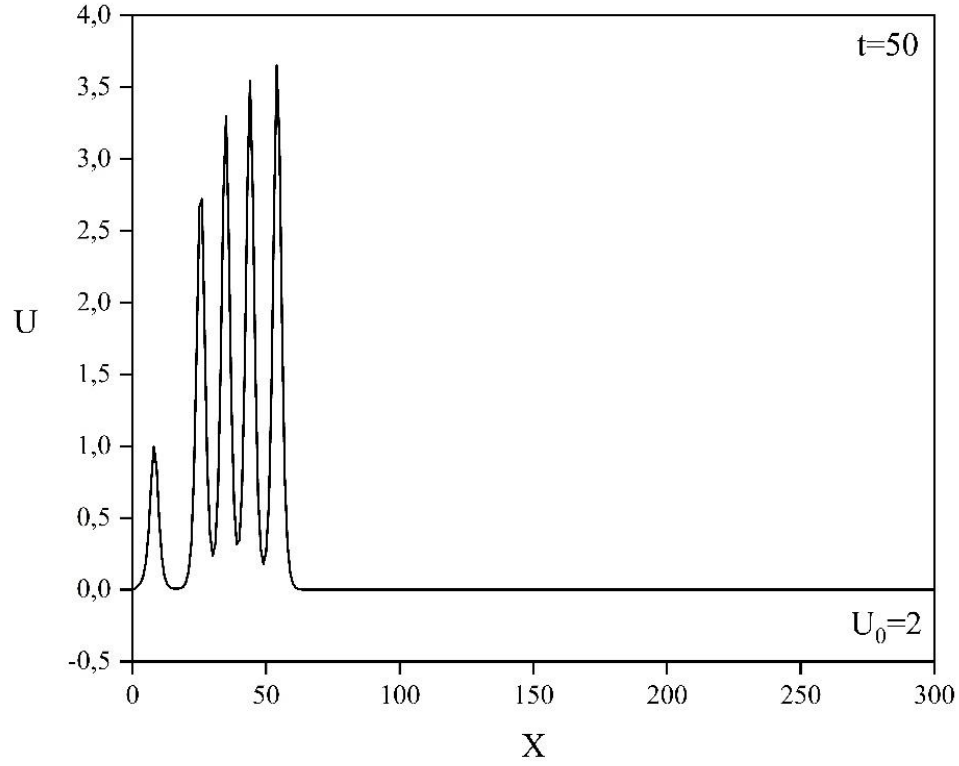
t=50
U
X
U_0=2
4,0
3,5
3,0
2,5
2,0
1,5
1,0
0,5
0,0
-0,5
0
50
100
150
200
250
300

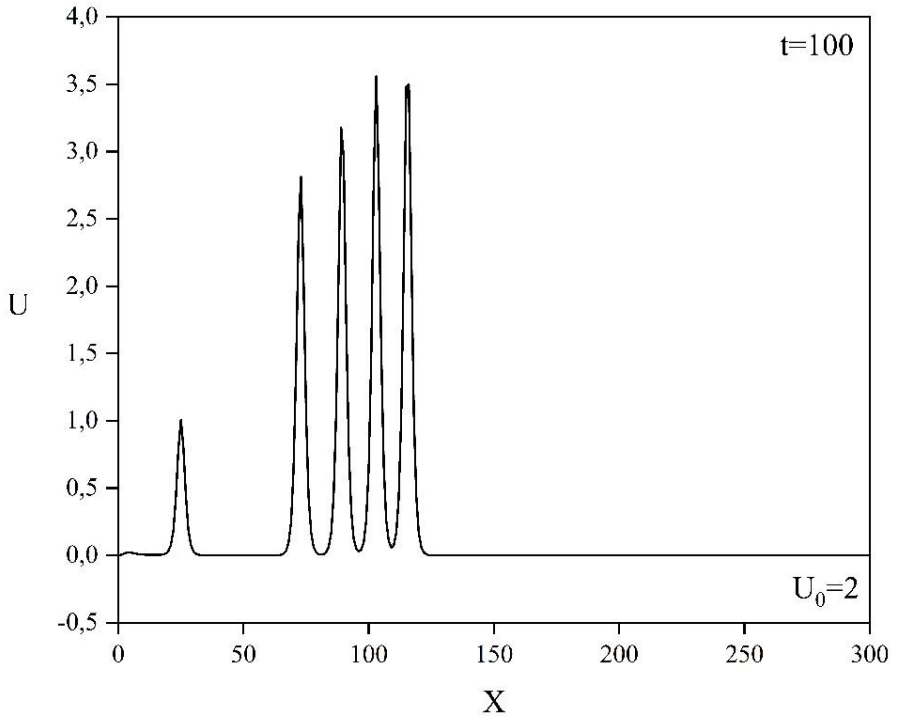

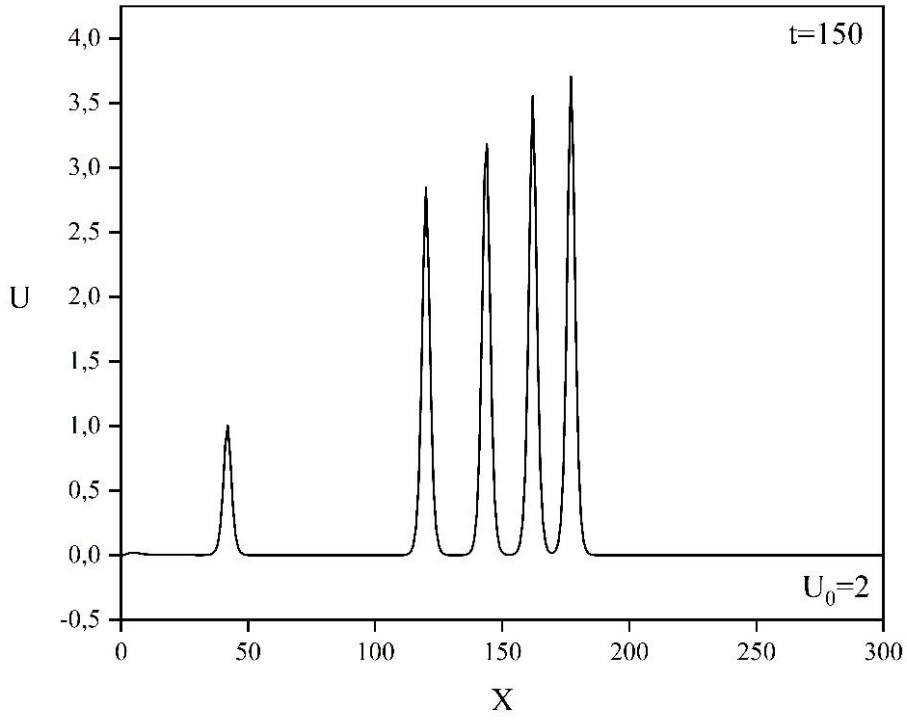

Figure 6: The boundary-forcing: $U_0 = 2$

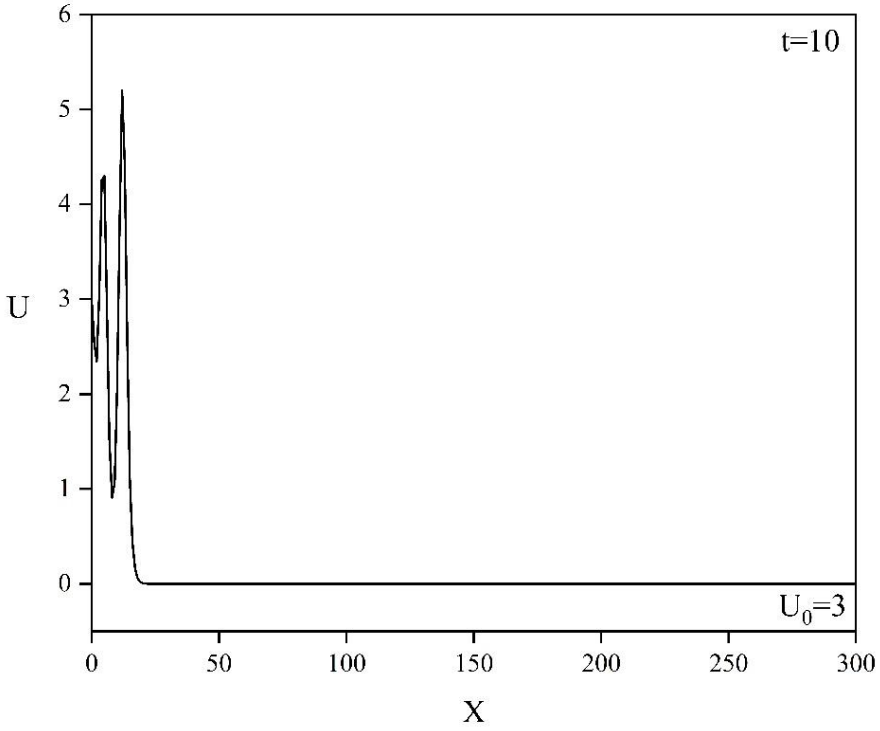
t=10
U
X
U_0=3
0
1
2
3
4
5
6
0
50
100
150
200
250
300

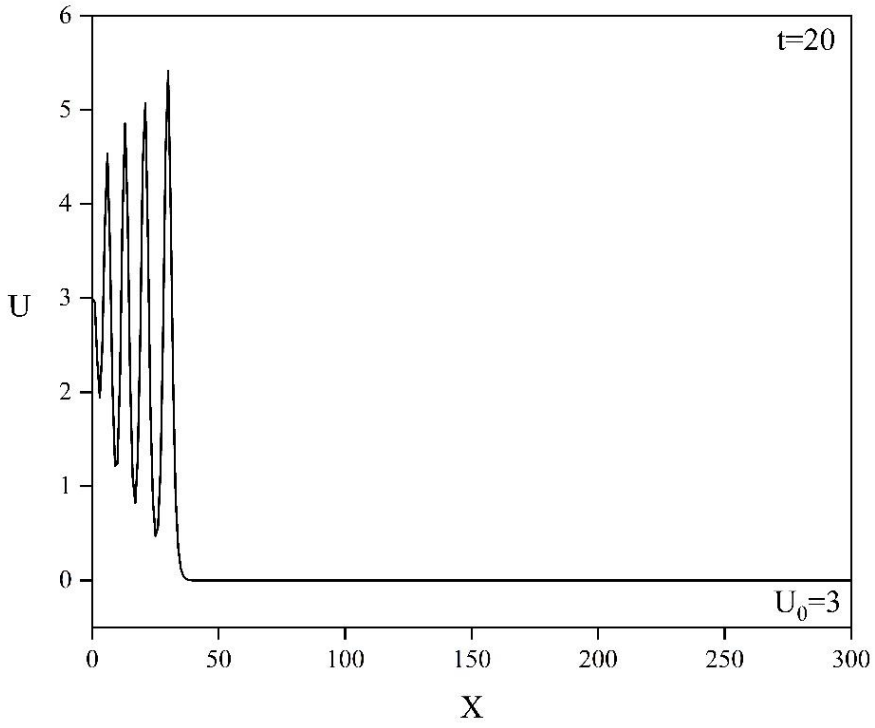
t=20
U
X
U_0=3
0
1
2
3
4
5
6
0
50
100
150
200
250
300

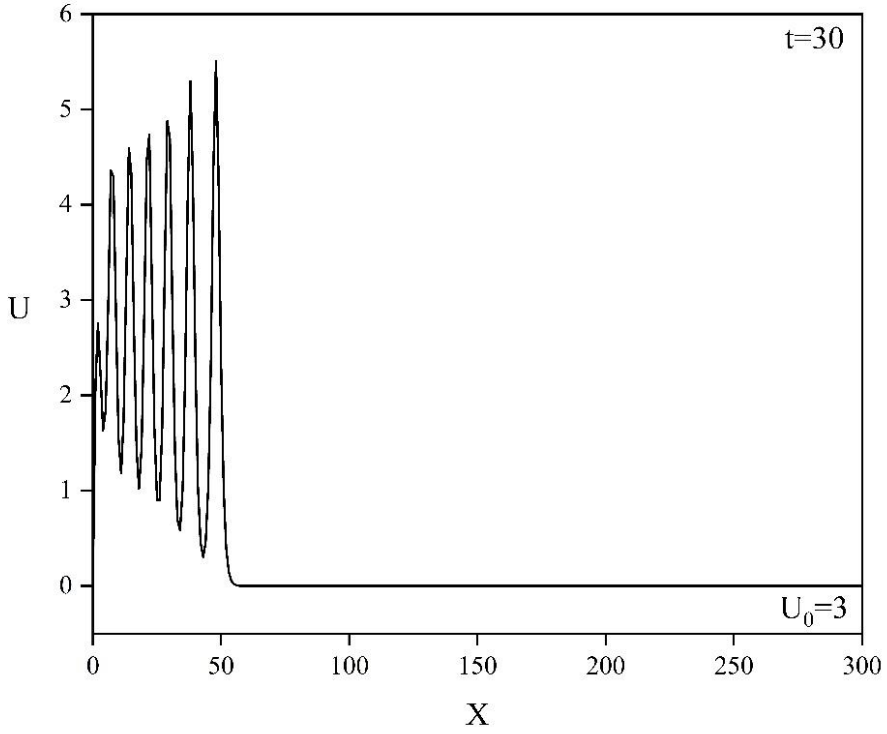
t=30
U
X
U_0=3
0
1
2
3
4
5
6
0
50
100
150
200
250
300

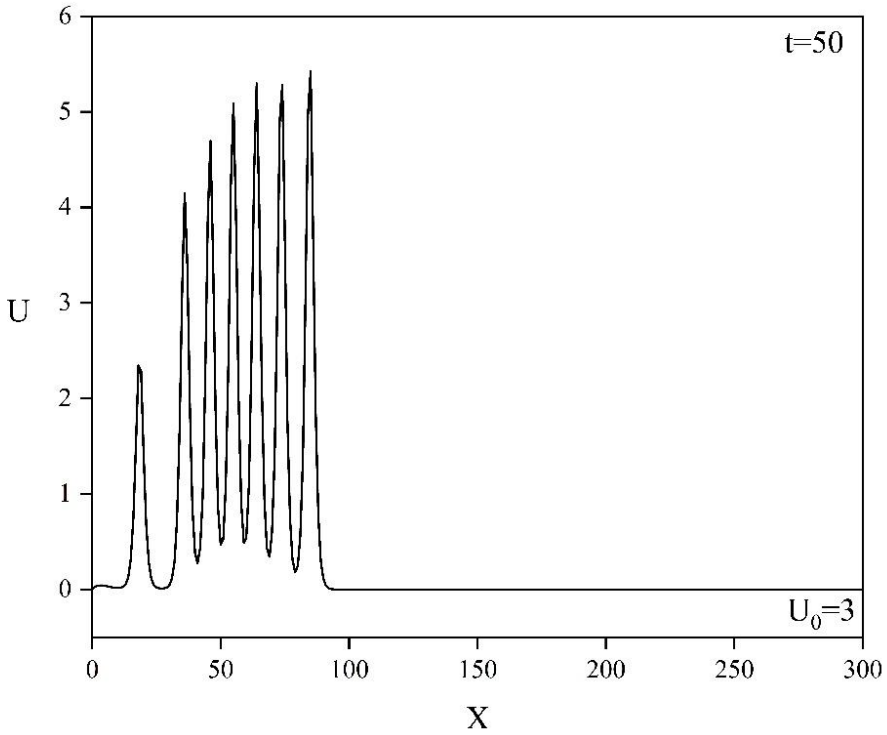
t=50
U
X
U_0=3
0
1
2
3
4
5
6
0
50
100
150
200
250
300

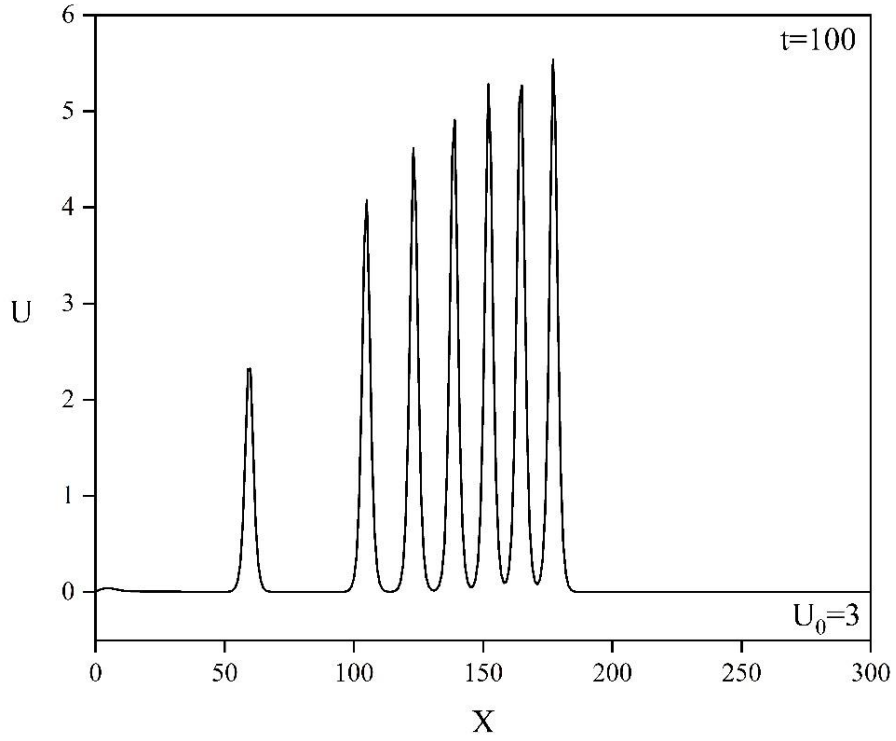

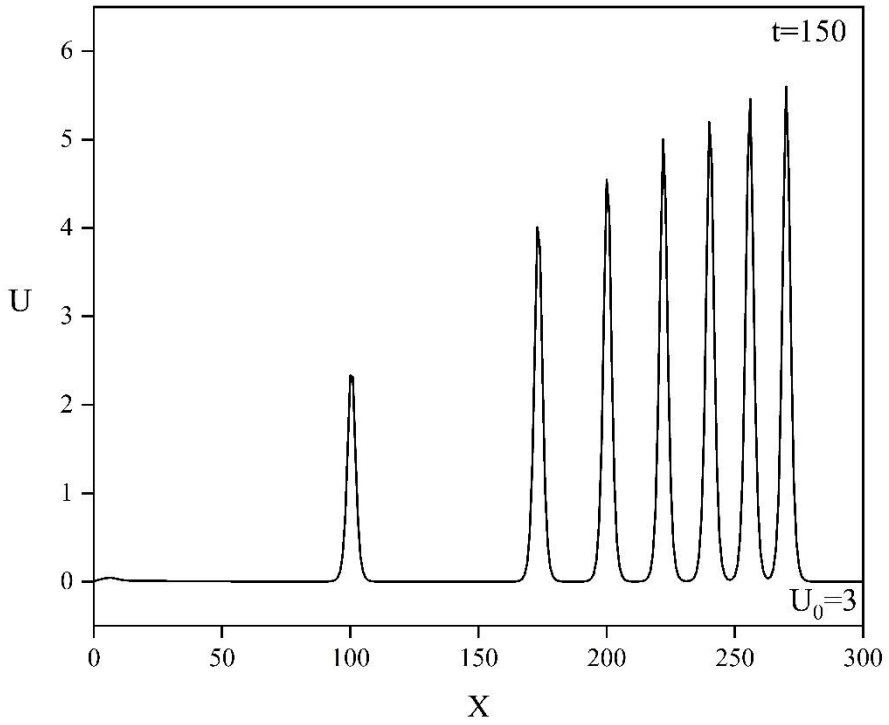

Figure 7: The boundary-forcing: $U_0 = 3$

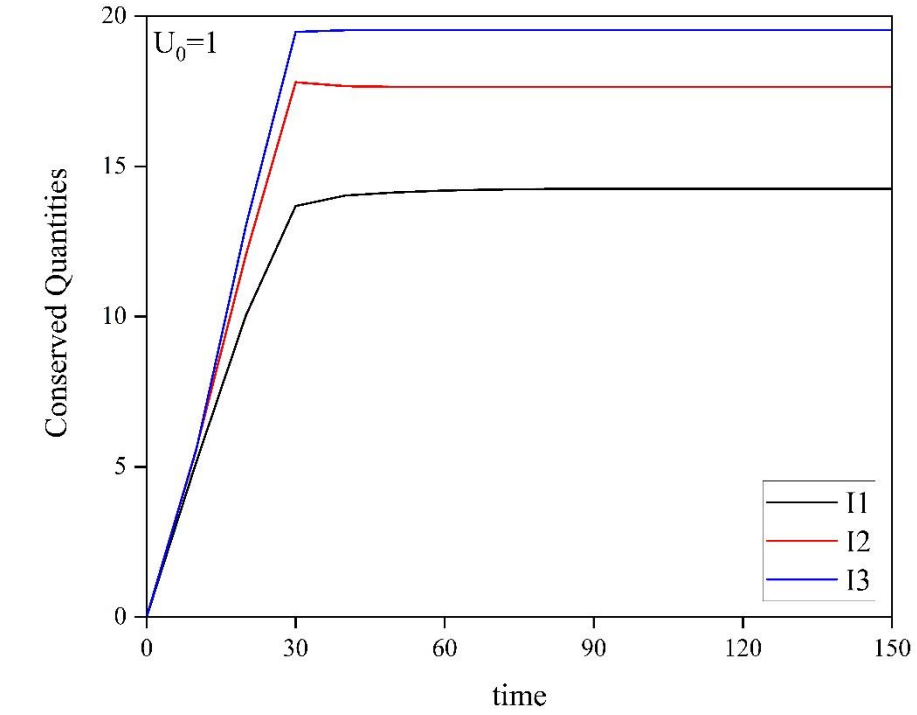
U_0=1
Conserved Quantities
time
I1
I2
I3
0
5
10
15
20
0
30
60
90
120
150

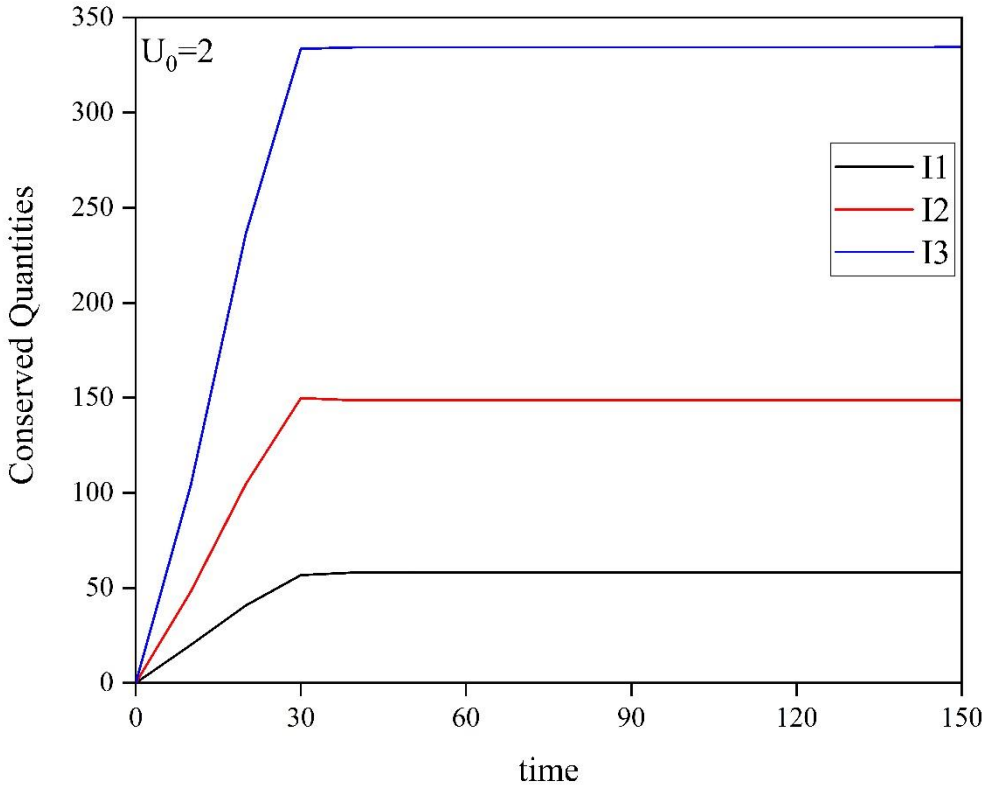
U_0=2
Conserved Quantities
time
I1
I2
I3
0
50
100
150
200
250
300
350
0
30
60
90
120
150

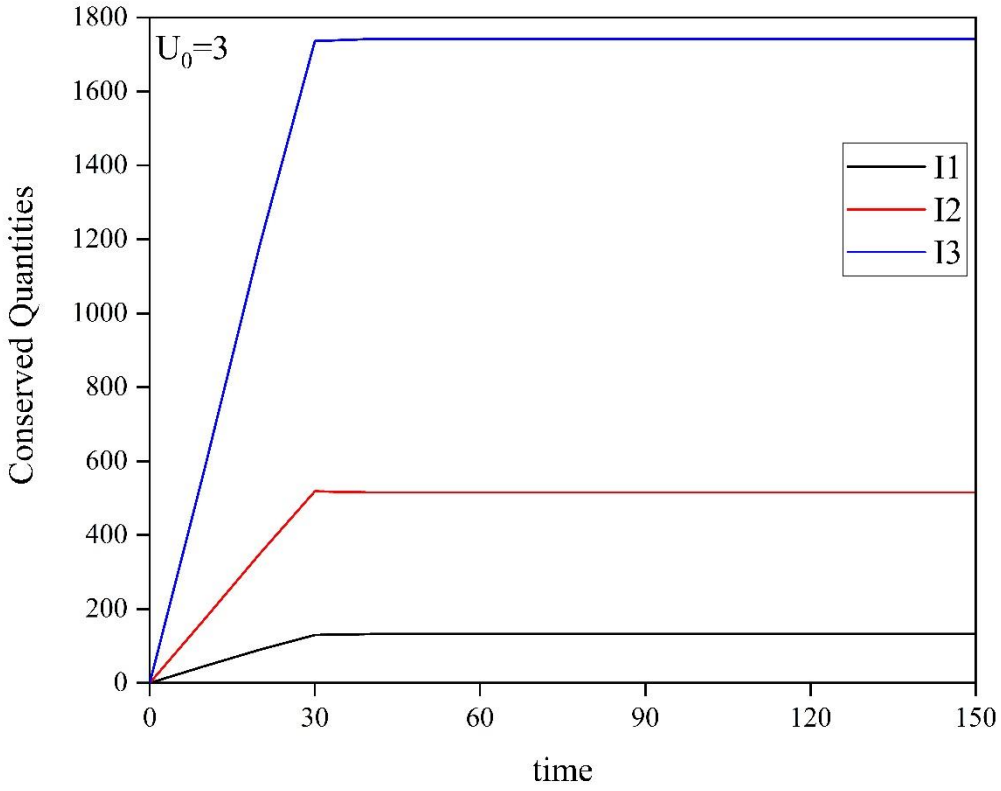

Figure 8: The invariants for boundary-forcing: $U_0 = 1, U_0 = 2, U_0 = 3$

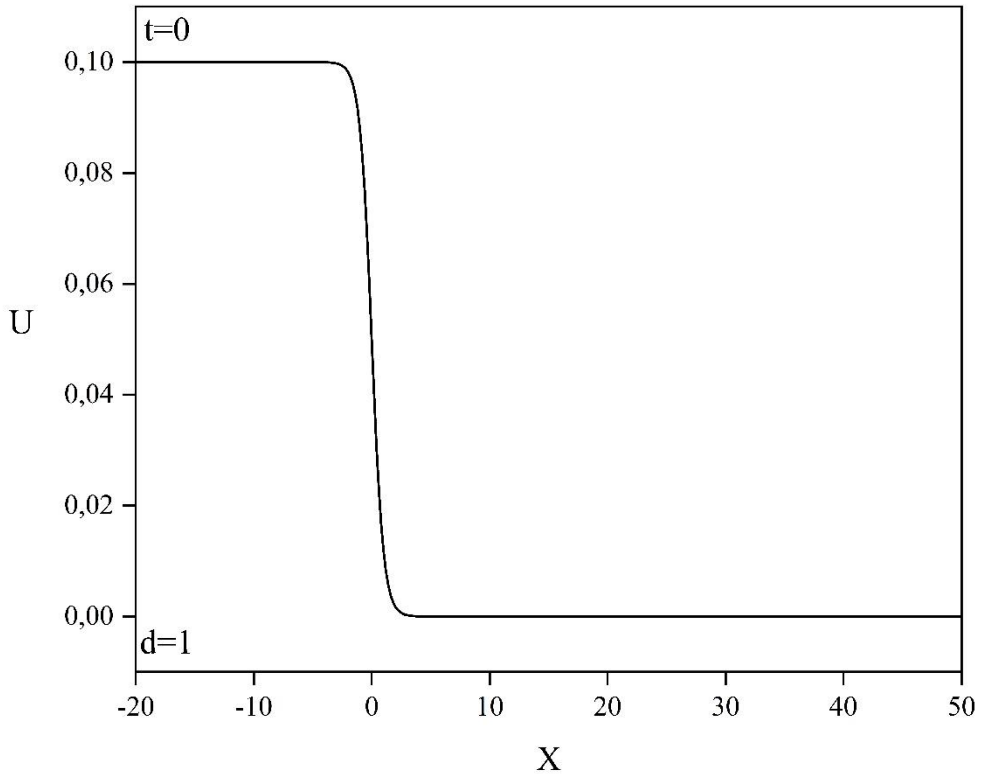
t=0
0,10
0,08
0,06
0,04
0,02
0,00
U
d=1
-20
-10
0
10
20
30
40
50
X

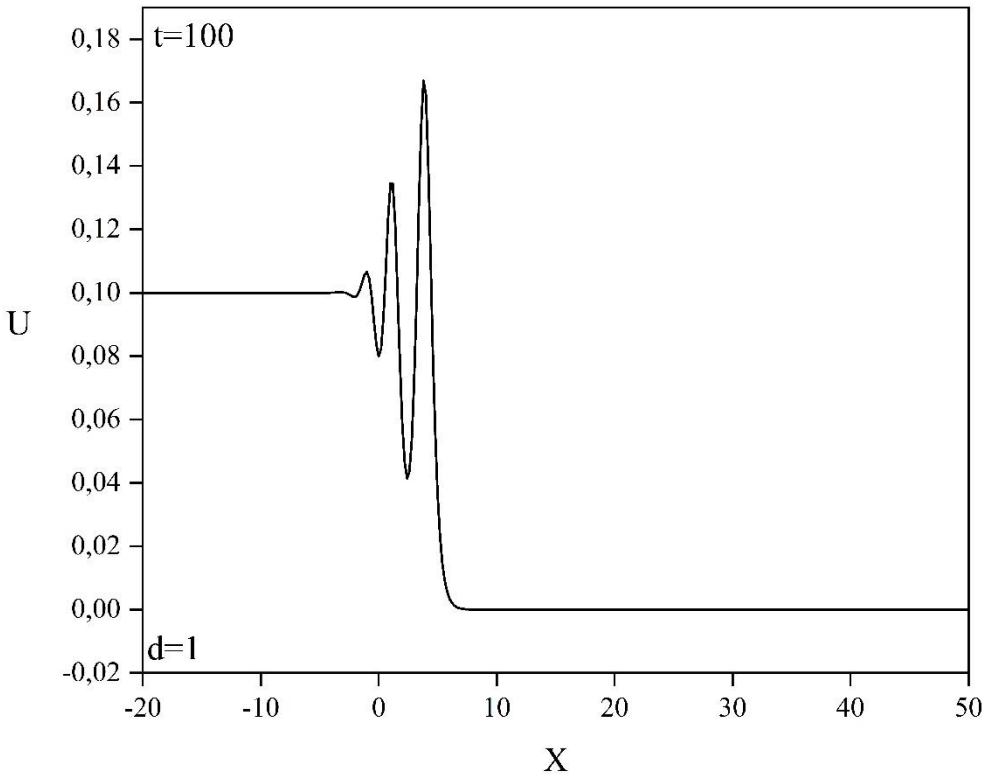
t=100
0,18
0,16
0,14
0,12
0,10
0,08
0,06
0,04
0,02
0,00
-0,02
U
d=1
-20
-10
0
10
20
30
40
50
X

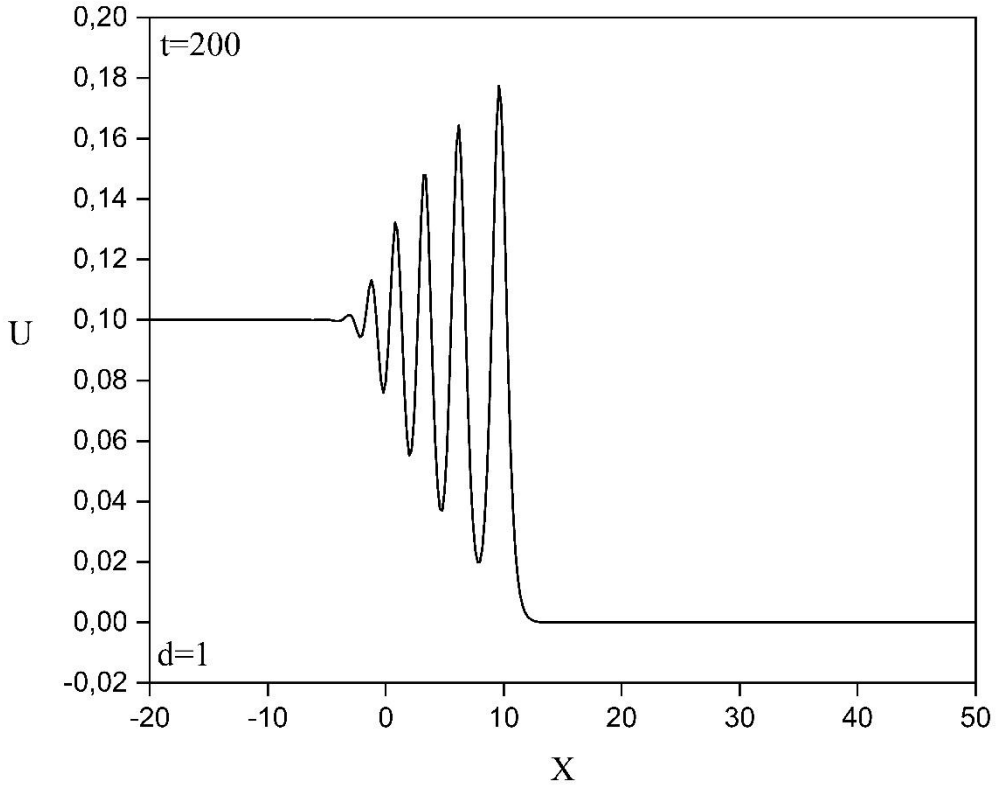
t=200
d=1
U
X
0,20
0,18
0,16
0,14
0,12
0,10
0,08
0,06
0,04
0,02
0,00
-0,02
-20
-10
0
10
20
30
40
50

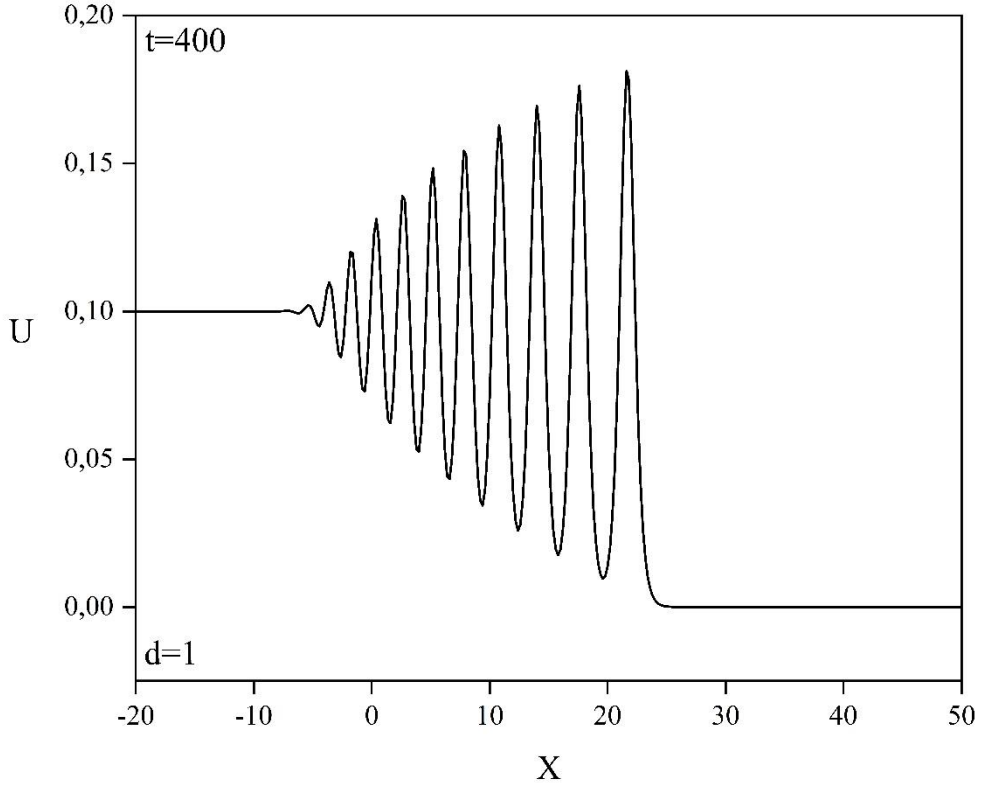
t=400
d=1
U
X
0,20
0,15
0,10
0,05
0,00
-20
-10
0
10
20
30
40
50

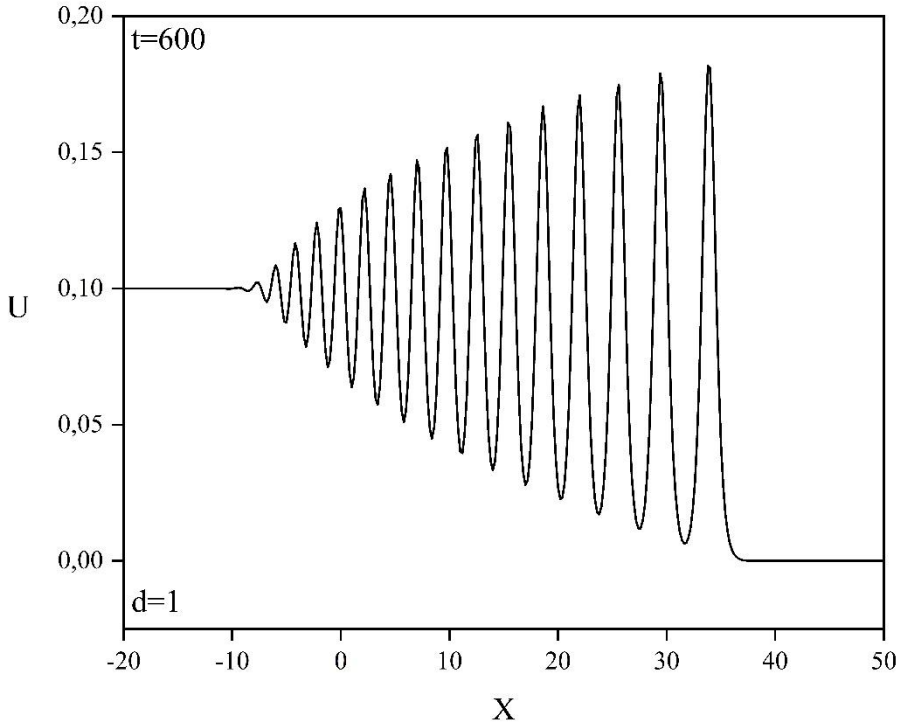

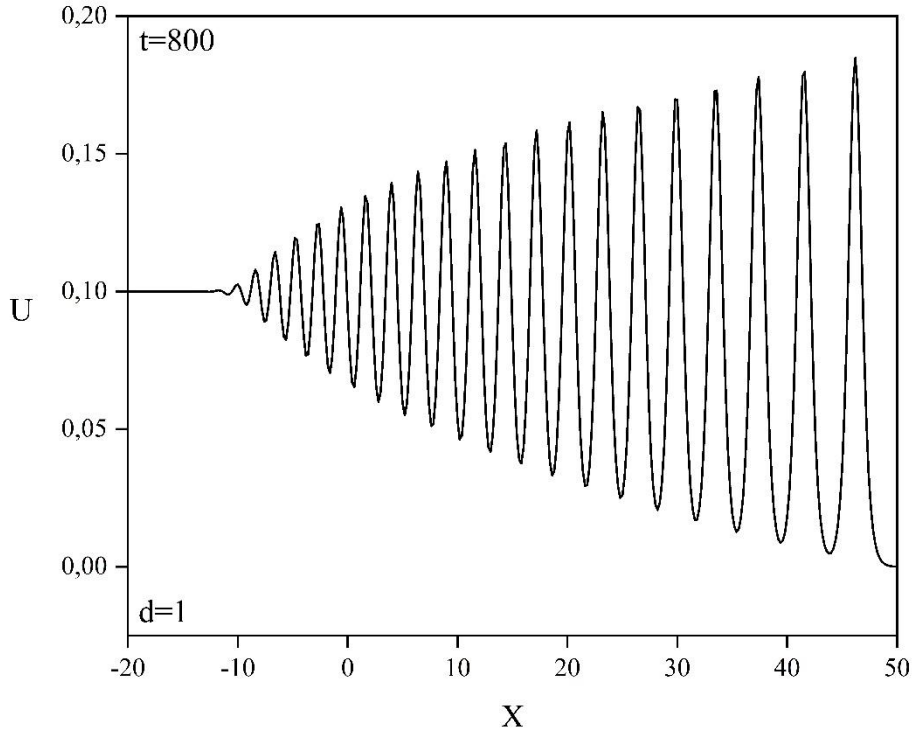

Figure 9: The wave undulation: $d = 1$

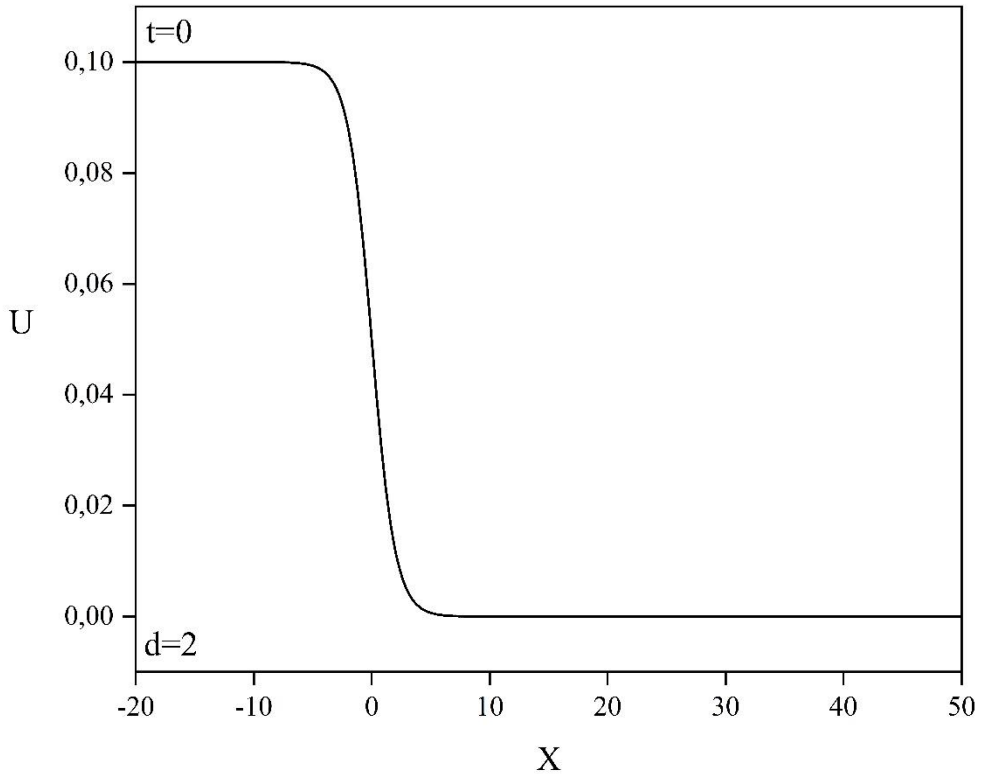
t=0
0,10
0,08
0,06
0,04
0,02
0,00
U
d=2
-20
-10
0
10
20
30
40
50
X

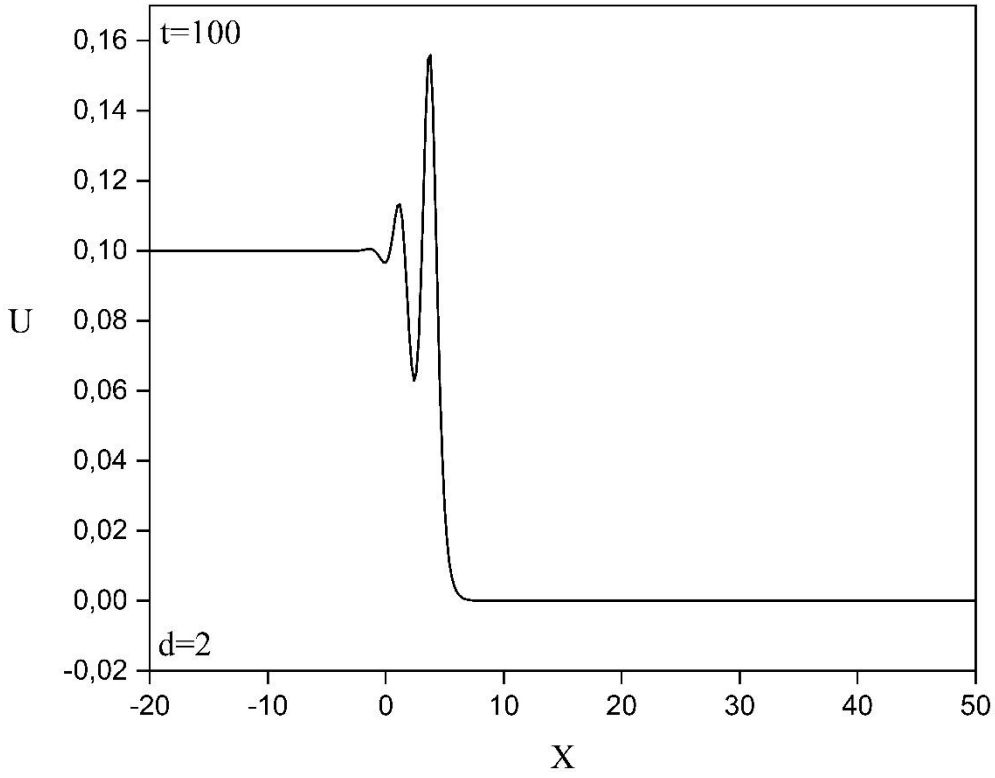
t=100
0,16
0,14
0,12
0,10
0,08
0,06
0,04
0,02
0,00
-0,02
U
d=2
-20
-10
0
10
20
30
40
50
X

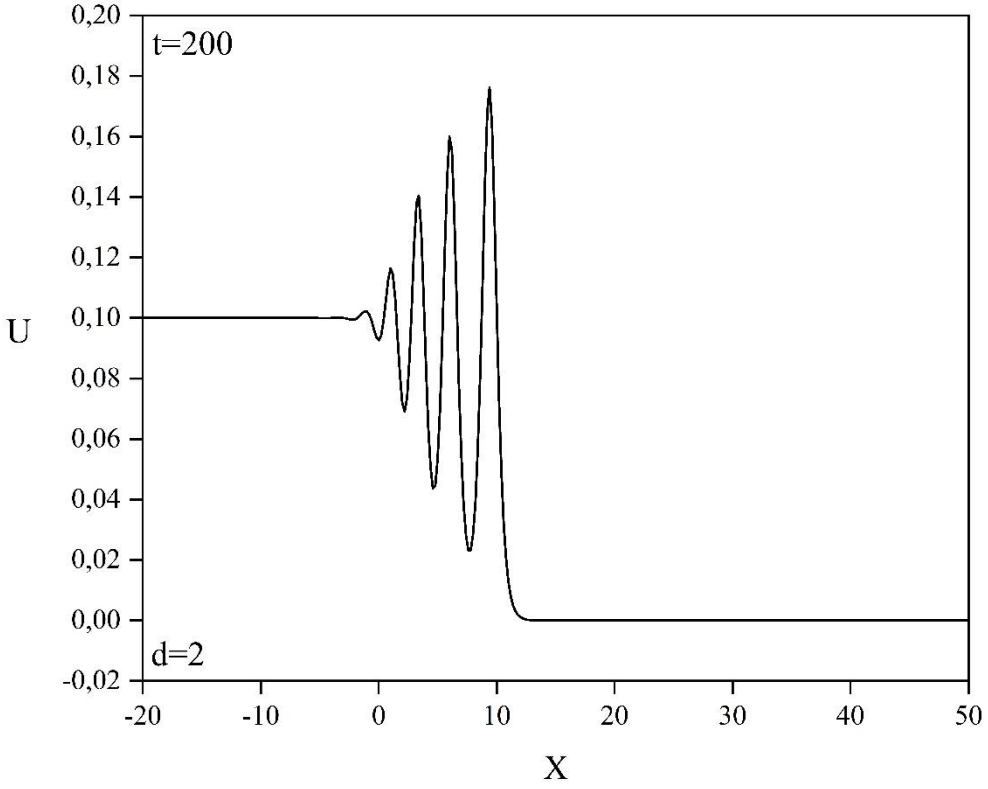
t=200
d=2
U
X
0,20
0,18
0,16
0,14
0,12
0,10
0,08
0,06
0,04
0,02
0,00
-0,02
-20
-10
0
10
20
30
40
50

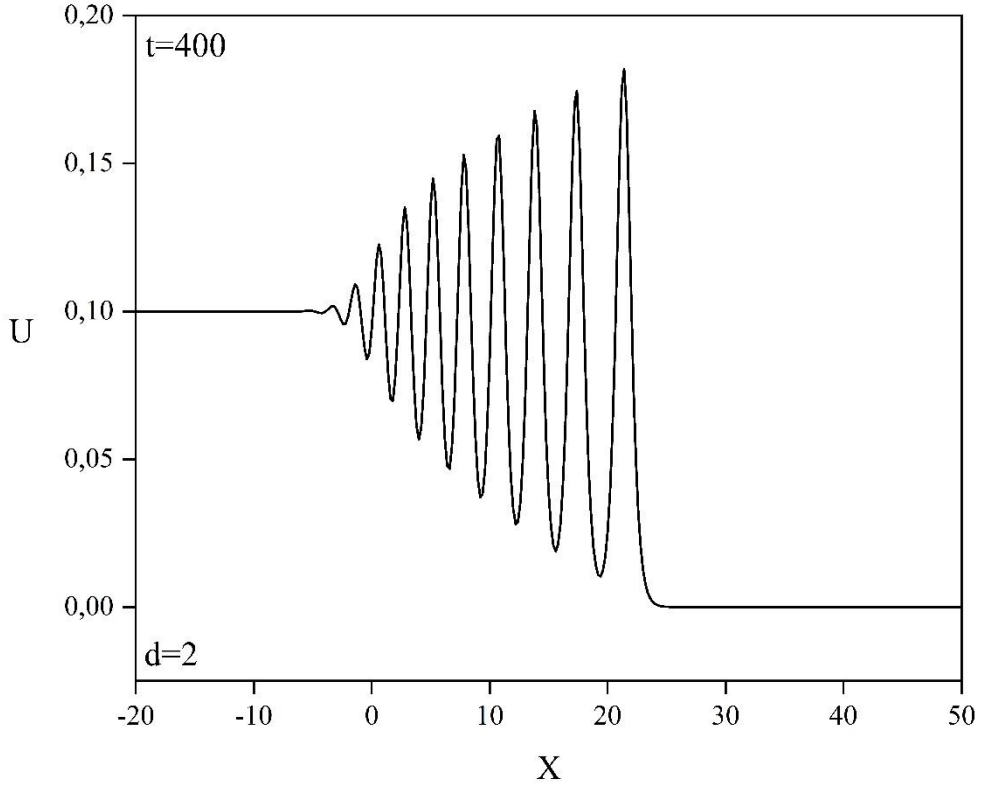
t=400
d=2
U
X
0,20
0,15
0,10
0,05
0,00
-20
-10
0
10
20
30
40
50

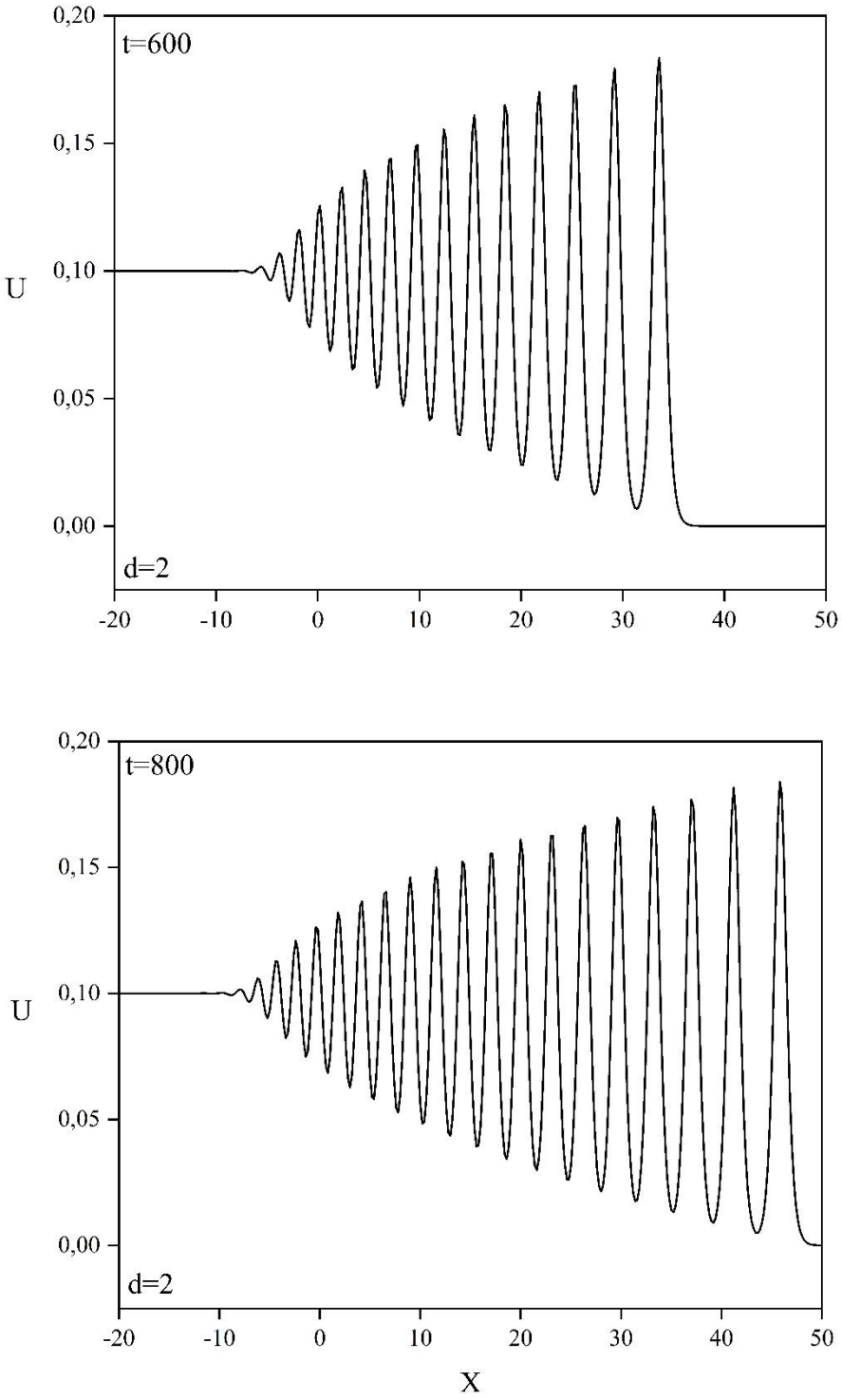

Figure 10: The wave undulation: $d = 2$

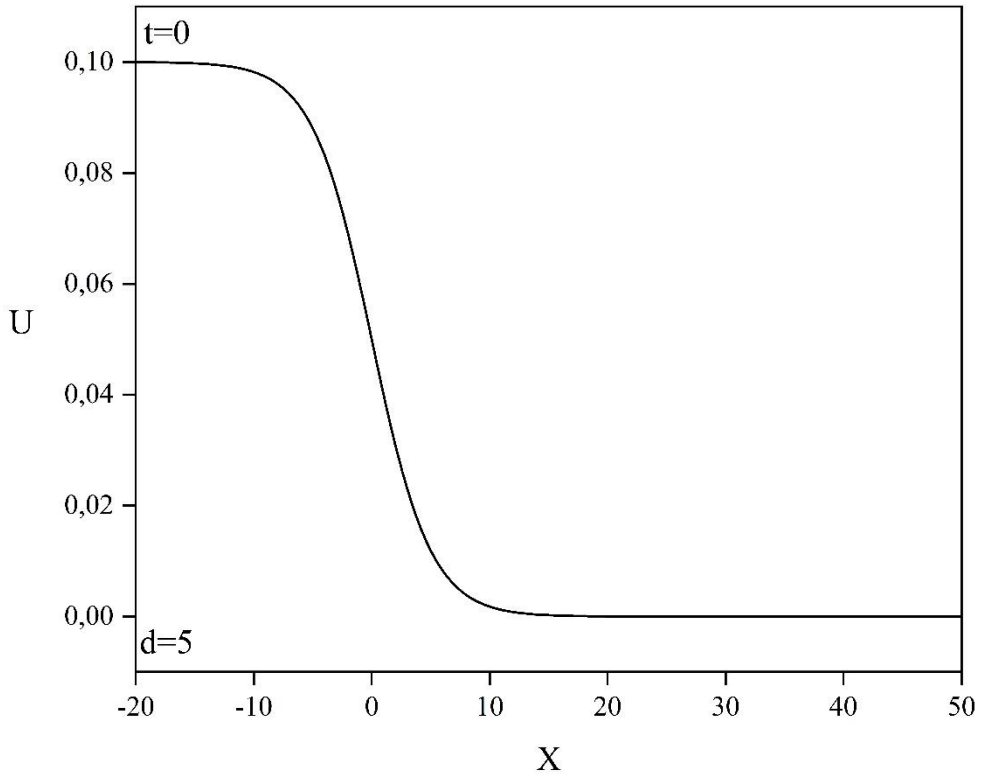
t=0
0,10
0,08
0,06
0,04
0,02
0,00
U
d=5
-20
-10
0
10
20
30
40
50
X

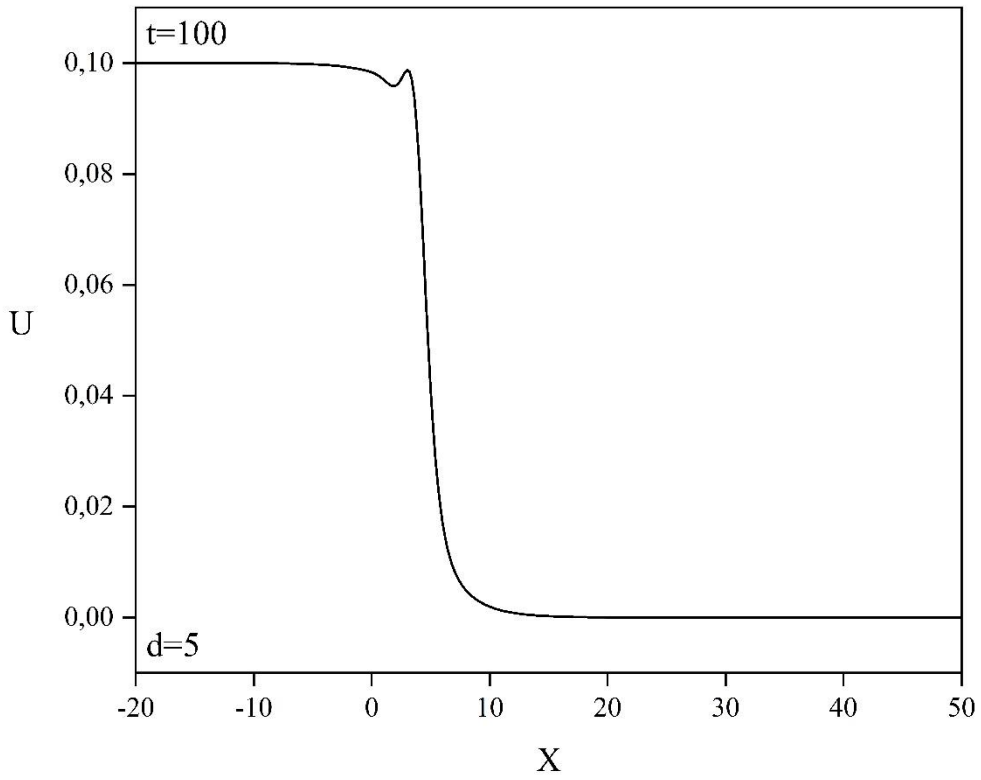
t=100
0,10
0,08
0,06
0,04
0,02
0,00
U
d=5
-20
-10
0
10
20
30
40
50
X

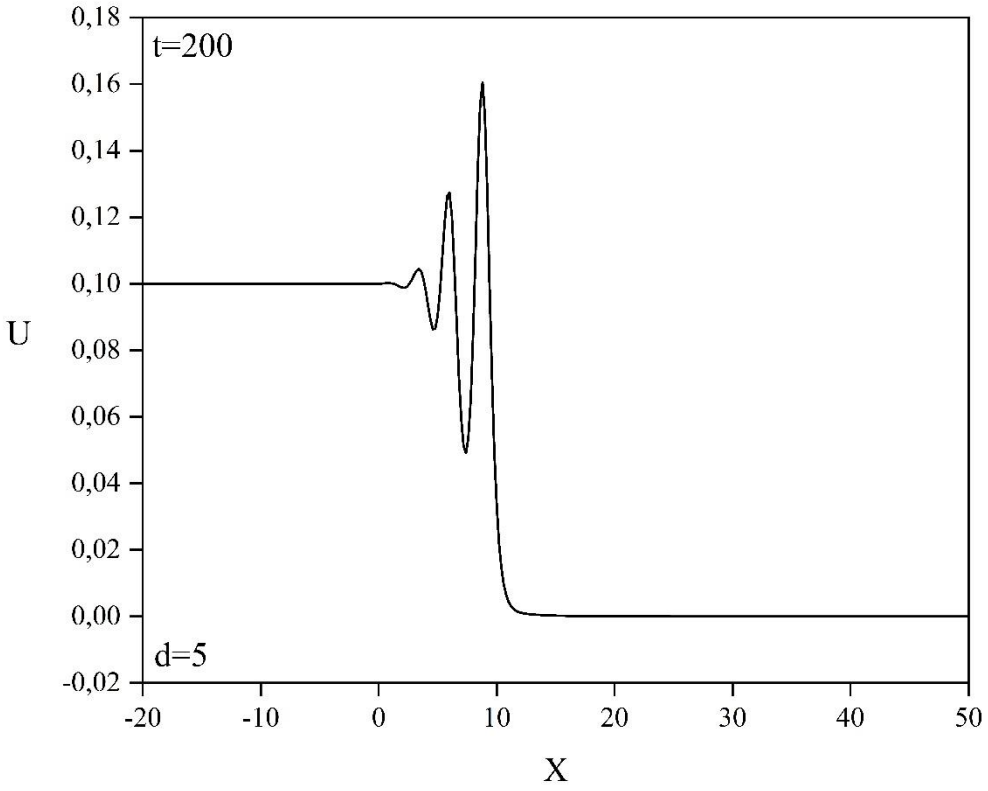
t=200
d=5
U
X
0,18
0,16
0,14
0,12
0,10
0,08
0,06
0,04
0,02
0,00
-0,02
-20
-10
0
10
20
30
40
50

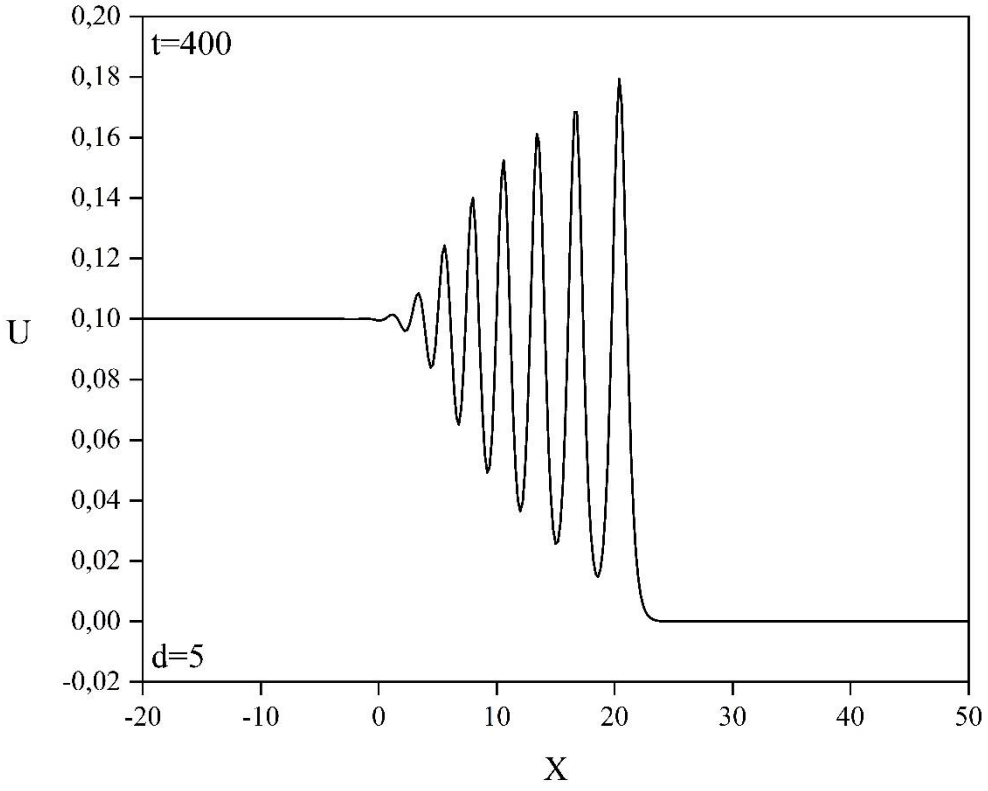
t=400
d=5
U
X
0,20
0,18
0,16
0,14
0,12
0,10
0,08
0,06
0,04
0,02
0,00
-0,02
-20
-10
0
10
20
30
40
50

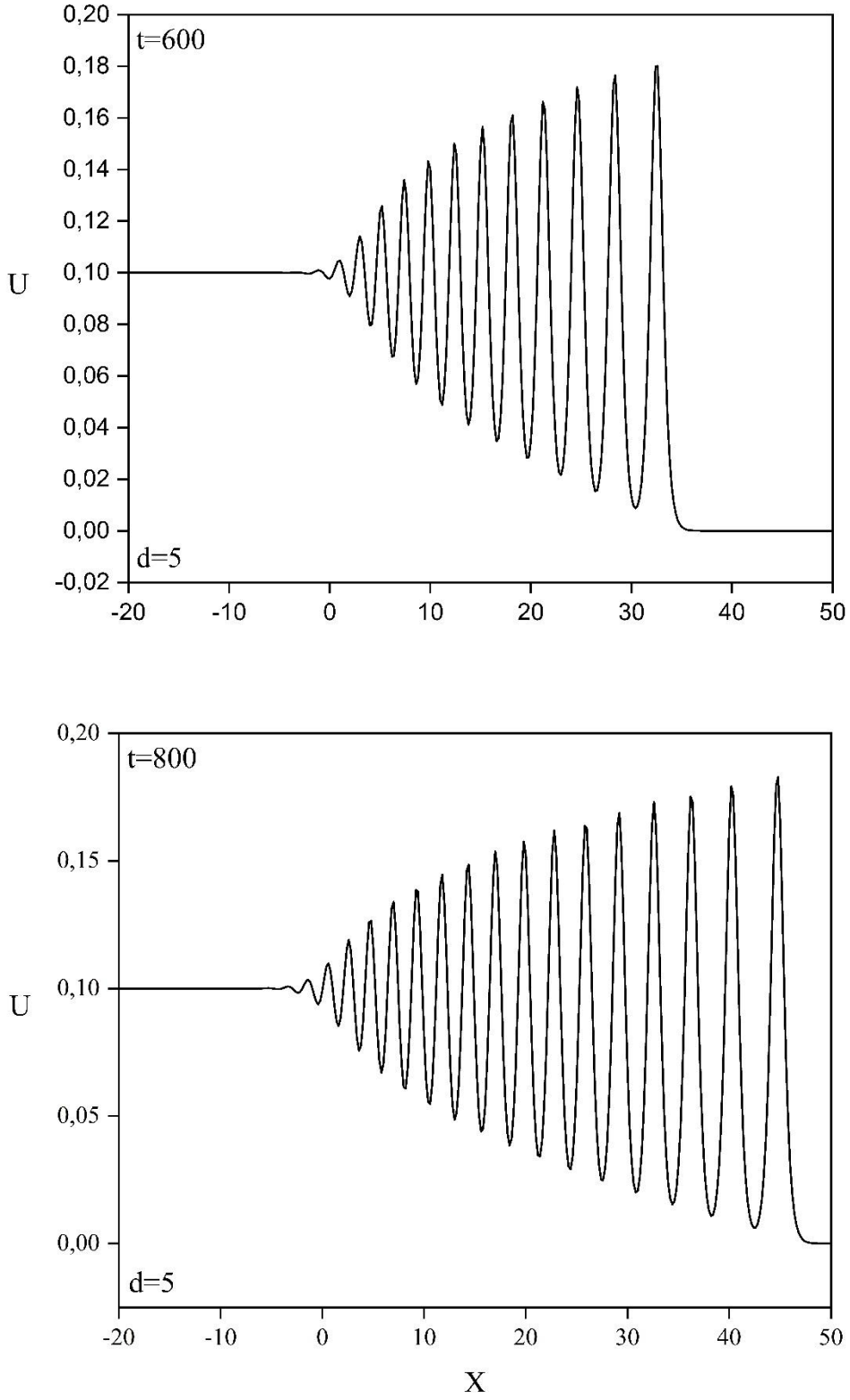

Figure 11: The wave undulation: $d = 5$

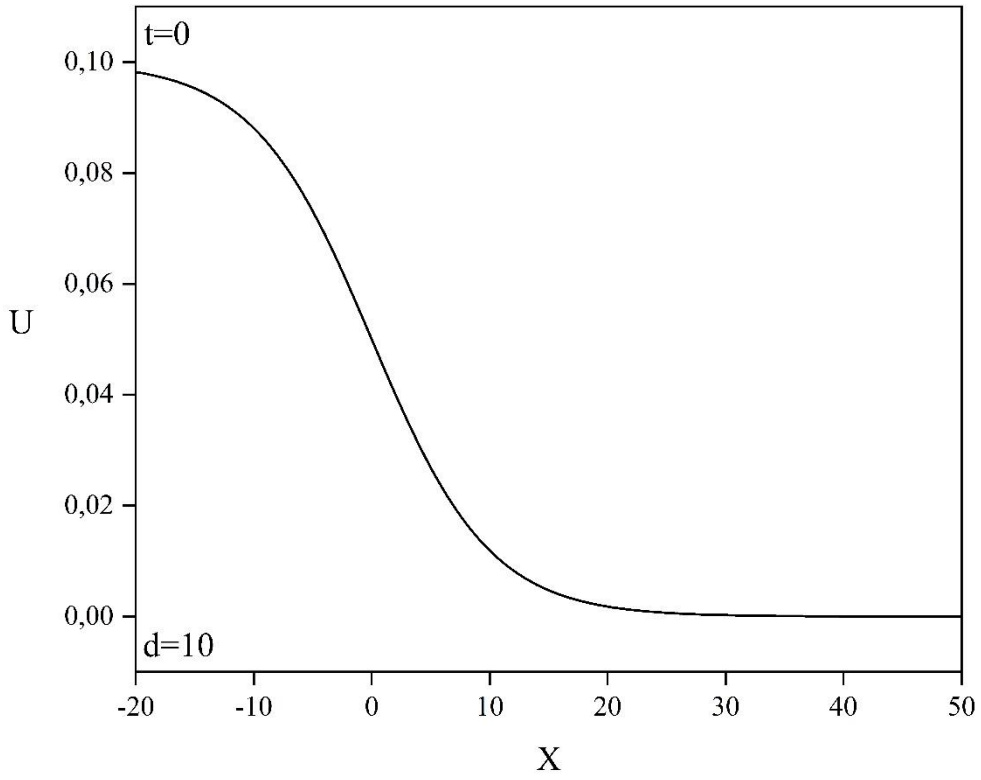
t=0
0,10
0,08
0,06
0,04
0,02
0,00
U
d=10
-20
-10
0
10
20
30
40
50
X

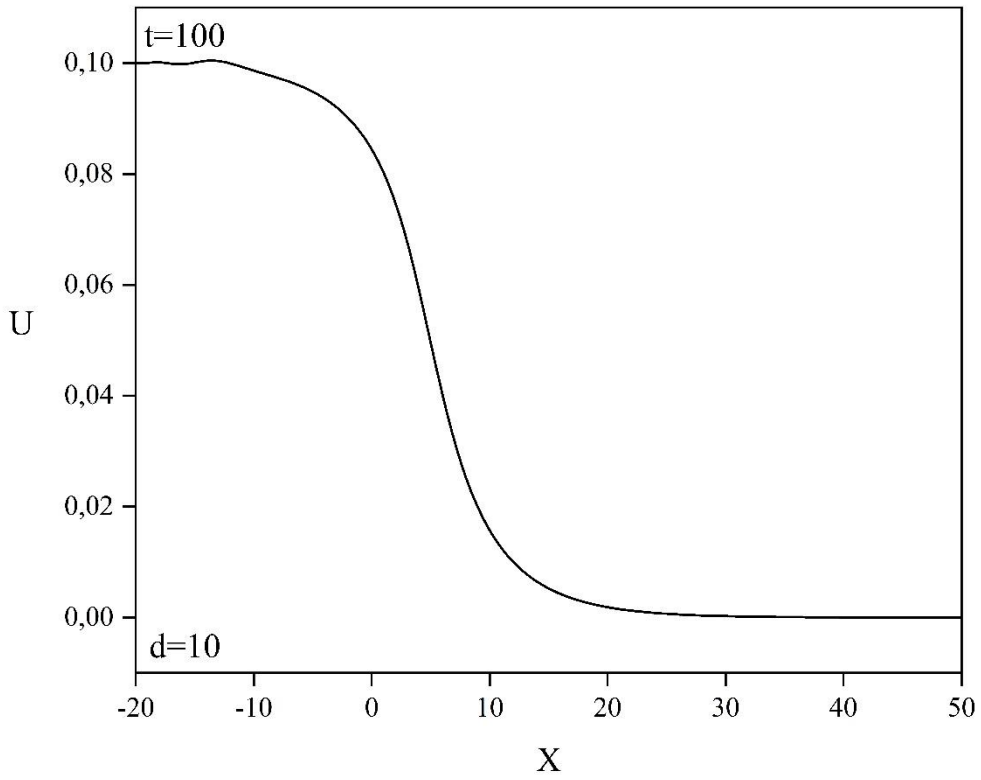
t=100
0,10
0,08
0,06
0,04
0,02
0,00
U
d=10
-20
-10
0
10
20
30
40
50
X

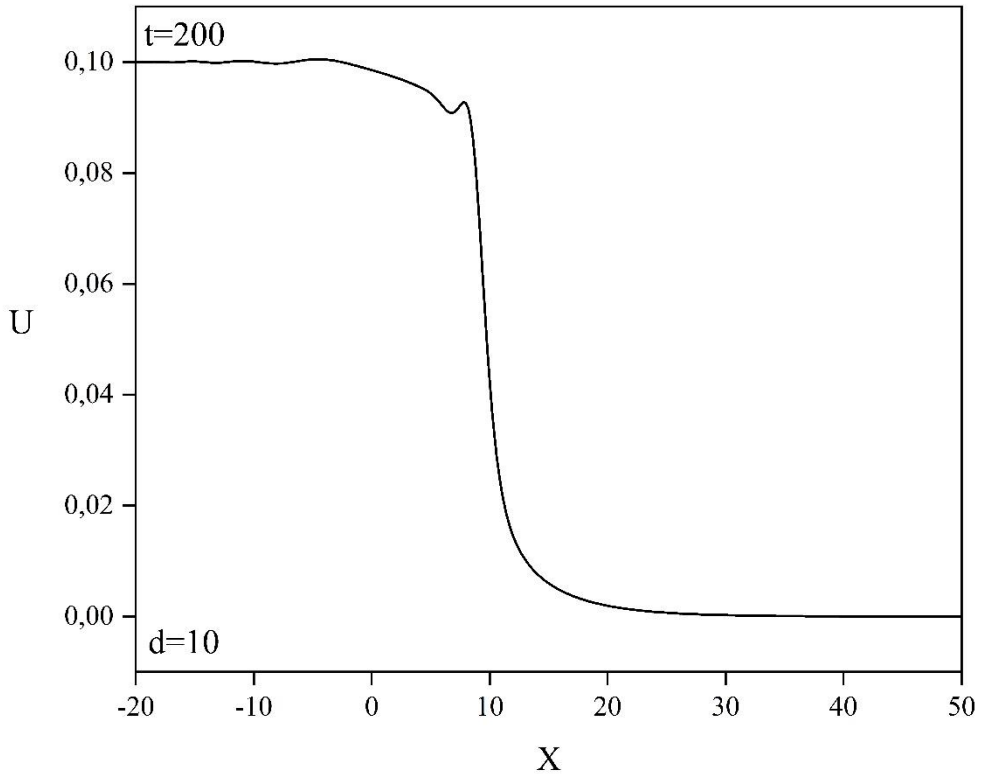
t=200
d=10
U
X
0,10
0,08
0,06
0,04
0,02
0,00
-20
-10
0
10
20
30
40
50

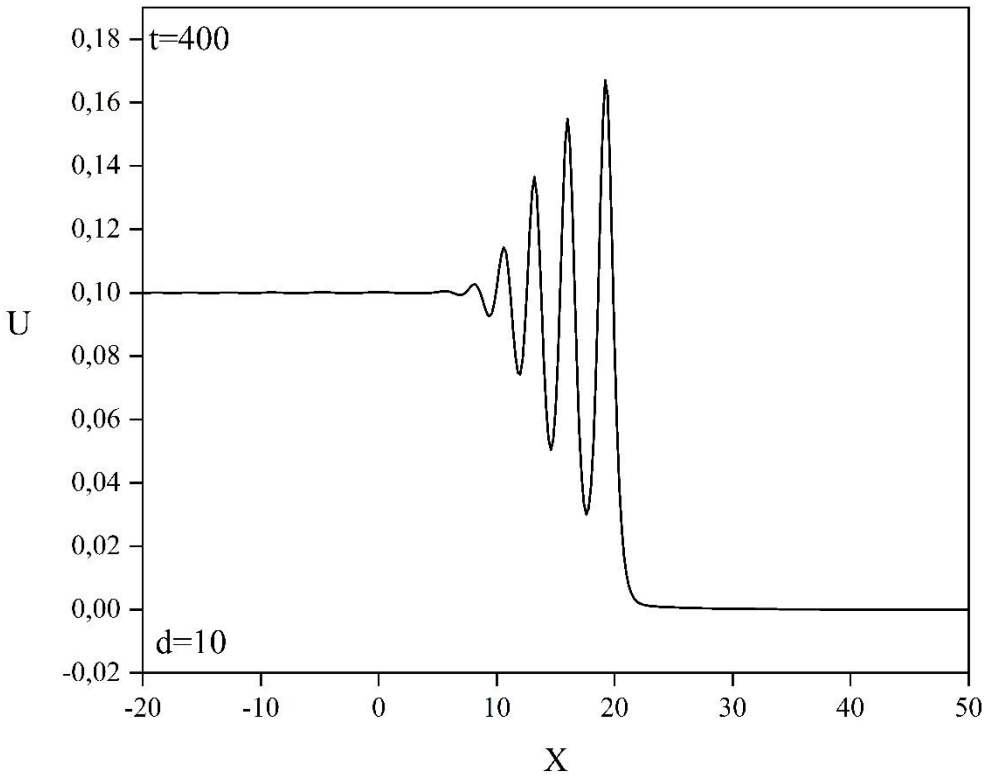
t=400
d=10
U
X
0,18
0,16
0,14
0,12
0,10
0,08
0,06
0,04
0,02
0,00
-0,02
-20
-10
0
10
20
30
40
50

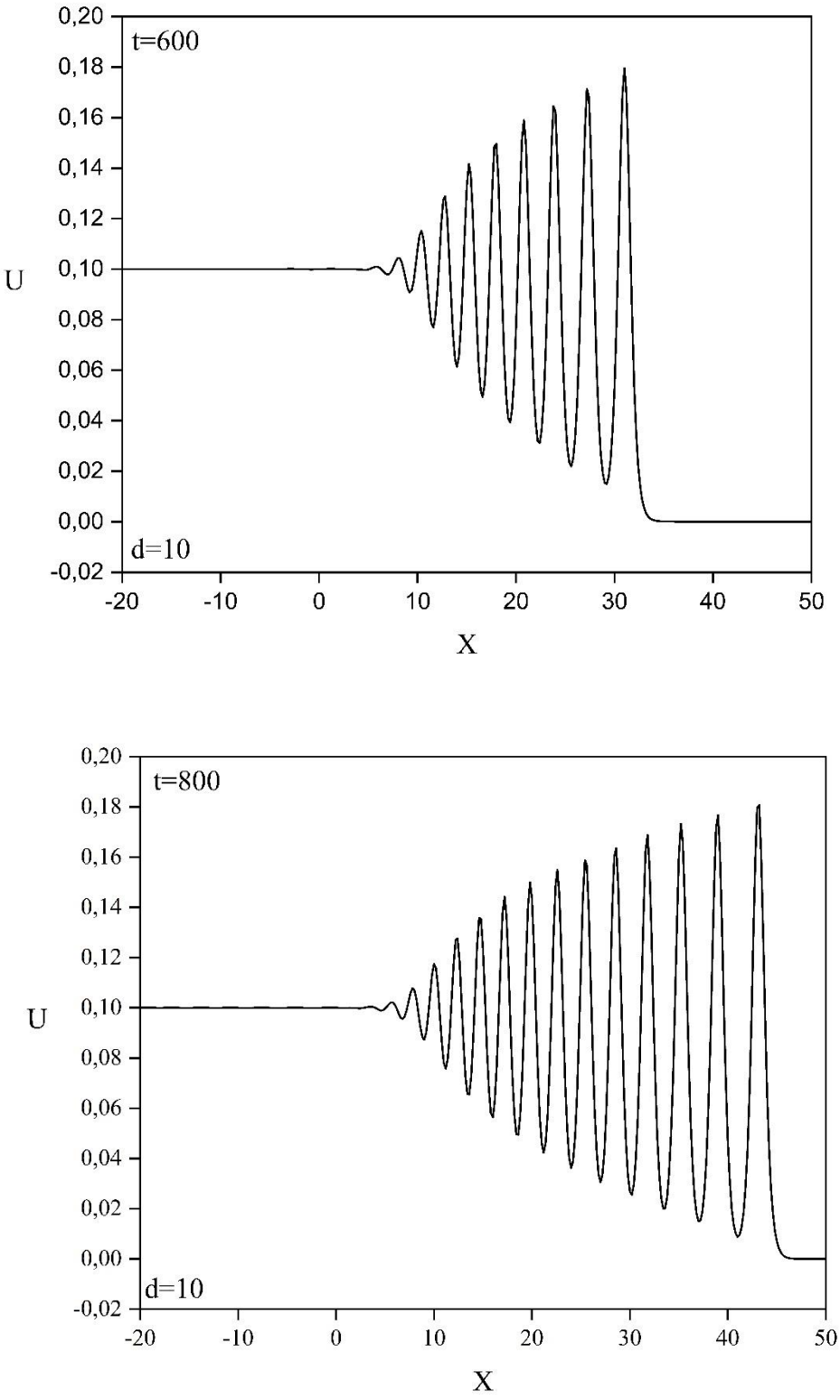

Figure 12: The wave undulation: $d = 10$

Table 1: Single solitary wave: $c = 1.0, \mu = 1, 0 \leq x \leq 80$.

Method	N	Δt	t	$L_2 \times 10^3$	$L_\infty \times 10^3$	I_1	I_2	I_3
DQM(Pres.)	1571	0.05	0	0.000	0.000	11.99999	28.79999	57.59996
			10	1.313	0.758	11.99998	28.80124	57.60366
			20	2.406	1.270	11.99947	28.79881	57.59649
			30	2.998	1.669	11.99987	28.80158	57.60478
			40	3.793	2.001	11.99946	28.79917	57.59746
PG [29]	1600	0.05	0	0.000	0.000	11.9994	28.8	57.6
			10	4.785	2.937	12.0	28.8	57.6
			20	7.211	4.287	12.0	28.8	57.6
			30	9.733	5.649	12.0	28.8	57.6
			40	12.294	7.016	12.0	28.8	57.6
Coll. [23]	2000	0.04	40	6.651	3.903	12.00137	28.80644	57.61935
	1600	0.05	40	17.189	9.359	11.99997	28.79944	57.59833
	1200	0.05	40	16.136	9.013	12.00021	28.80143	57.60430
	800	0.1	40	63.380	34.677	12.00023	28.80085	57.60250
	400	0.1	40	95.670	53.915	12.00010	28.80053	57.60130
	800	0.2	40	222.500	119.881	12.00050	28.80165	57.60463
	400	0.2	40	252.869	138.091	12.00060	28.80230	57.60610
Gal. [13]	2000	0.04	40	7.514	-	11.9935	28.8177	57.6549
	1600	0.05	40	37.365	-	11.9977	28.7842	57.5548
	800	0.1	40	68.558	-	12.0079	28.8247	57.6826
	400	0.2	40	218.173	-	12.0474	28.9512	58.0881
PG [28]	2000	0.04	40	24.6	-	12.0157	28.8660	57.7996
	1600	0.05	40	5.4	-	12.0119	28.8416	57.7270
	1200	0.05	40	33.0	-	11.9972	28.7884	57.5692
	800	0.1	40	91.7	-	12.0003	28.7976	57.6014
	400	0.1	40	123.8	-	12.0001	28.7895	57.6018
	800	0.2	40	339.0	-	11.9999	28.7965	57.5981
	400	0.2	40	367.2	-	12.0001	28.7891	57.6011
MOL [32]	2000	0.04	40	15.4	-	12.0000	28.7995	57.6
	1600	0.05	40	24.1	-	12.0000	28.7993	57.6
	800	0.1	40	96.5	-	12.0000	28.7971	57.5998
	400	0.2	40	386.2	-	12.0000	28.7868	57.5944
Analytic						12.00000	28.80000	57.60000

Table 2: Error norms and rates of convergence at $t = 40 : c = 1.0, \mu = 1,\ 0 \leq x \leq 80$.

Method	N	$L_2 \times 10^3$	ROC	$L_\infty \times 10^3$	ROC
Present	241	26.524	-	13.997	-
	481	20.089	0.402	10.610	0.401
	981	16.884	0.243	8.922	0.243
	1291	12.535	1.084	6.743	1.020
	1571	3.793	6.089	2.001	6.189

Table 3: Single solitary wave: $c = 0.1, \mu = 1,\ 0 \le x \le 30$.

Method	N	Δt	t	$L_2\times10^3$	$L_\infty\times10^3$	I_1	I_2	I_3
DQM(Pres.)	261	0.05	0	0.000000	0.000000	1.199948	0.288000	0.057600
			10	0.015089	0.020041	1.199960	0.287999	0.057600
			20	0.006261	0.007373	1.199980	0.287999	0.057600
			30	0.004022	0.003504	1.199989	0.288000	0.057600
			40	0.005138	0.003361	1.199989	0.287996	0.057599
			50	0.005324	0.003527	1.199991	0.287996	0.057599
			60	0.006455	0.004052	1.199993	0.287996	0.057599
			70	0.006413	0.003664	1.199994	0.287998	0.057600
			80	0.008143	0.006568	1.199983	0.287997	0.057599
Gal. [12]	1000	0.05	80	0.040	0.024	1.19998	0.28800	0.05759
Gal. [13]	1000	0.05	80	24.697	16.425	1.23387	0.29915	0.06097
Coll. [17]	1000	0.05	80	0.03962	0.05446	1.20004	0.28800	0.05760
Coll. [21]	1000	0.05	80	0.062	0.053	1.200047	0.288000	0.057600
Coll. [22]	1000	0.05	80	0.0490	0.0336	1.199994	0.28800	0.05756
Coll. [24]p=1	1000	0.05	80	0.089	0.054	1.1999	0.2878	0.0576
Coll. [24] p=0.0000340714	1000	0.05	80	0.017	0.0073	1.1999	0.2880	0.0576
Coll. [24]p=1	2000	0.05	80	1.9	1.2	1.1999	0.2880	0.0576
Coll. [24] p=0.0000039997	2000	0.05	80	0.59	0.26	1.2000	0.2880	0.0576
Coll. [25]		0.05	80	0.022685	0.012647	1.19999	0.28799	0.05759
PG [28]	1000	0.05	80	3.849	2.646	1.1910	0.2855	0.05582
PG [29]	1000	0.05	80	0.038815	0.051514	1.20004	0.288	0.0576
Lum.Gal. [35]	1000	0.05	80	0.029	0.021	1.19995	0.28798	0.05759
FIFDM [36]	1000	0.05	80	0.12476	0.07254	1.20004	0.28800	0.05760
RBF-PS. [33] RK4(MQ)	200	0.05	80	0.01306	0.007373	1.19399	0.28656	0.05731
RBF-PS. [33] RK4$(\emptyset_{2,3})$	200	0.05	80	0.02301	0.007373	1.19399	0.28656	0.05731
RBF-PS. [33] ode113(MQ)	200	0.05	80	0.05343	0.01363	1.19399	0.28656	0.05731
RBF-PS. [33] ode113$(\emptyset_{2,3})$	200	0.05	80	0.04813	0.01362	1.19399	0.28656	0.05731
FDM. [34]	250	0.05	80	1.84643	1.12832	-	-	-
	500	0.05	80	0.46614	0.28405	-	-	-
	1000	0.05	80	0.12476	0.07254	-	-	-
	2000	0.05	80	0.05031	0.05365	-	-	-
MOL. [32]	1000	0.05	80	0.183785	0.095878	1.20004	0.287997	0.0576
OS. [37] A-B	600	0.05	80	0.057386	0.052850	1.200041	0.288000	0.057600
OS. [37] B-A	600	0.05	80	0.057386	0.052850	1.200041	0.288000	0.057600
OS. [37] A-B-A	600	0.05	80	0.057386	0.052850	1.200041	0.288000	0.057600
OS. [37] B-A-B	600	0.05	80	0.054761	0.052850	1.200041	0.288000	0.057600
Analytic						1.200000	0.288000	0.057600

Table 4: Single solitary wave: $c = 0.03, \mu = 1,\ 0 \le x \le 30$.

Method	N	Δt	t	$L_2\times10^3$	$L_\infty\times10^3$	I_1	I_2	I_3
DQM(Pres.)	165	0.05	0	0.000000	0.000000	0.359985	0.025920	0.001555
			10	0.009388	0.012107	0.359977	0.025920	0.001555
			20	0.006973	0.008969	0.359983	0.025920	0.001555
			30	0.005183	0.006645	0.359986	0.025920	0.001555
			40	0.003948	0.004923	0.359991	0.025920	0.001555
			50	0.003081	0.003647	0.359995	0.025920	0.001555
			60	0.002315	0.002702	0.359996	0.025920	0.001555
			70	0.001721	0.002001	0.359996	0.025920	0.001555
			80	0.001433	0.001483	0.359997	0.025920	0.001555
Gal. [13]	600	0.05	0	0.004	0.016	0.35998	0.02592	0.00156
			10	0.285	0.152	0.36081	0.02600	0.00156
			20	0.579	0.329	0.36164	0.02608	0.00157
			30	0.884	0.529	0.36247	0.02616	0.00158
			40	1.204	0.750	0.36330	0.02625	0.00159
			50	1.541	0.993	0.36413	0.02633	0.00159
			60	1.898	1.255	0.36497	0.02641	0.00160
			70	2.278	1.536	0.36581	0.02649	0.00161
			80	2.683	1.836	0.36665	0.02658	0.00162
MOL[32]	600	0.05	80	0.0471519	0.0247077	0.360013	0.0259194	0.0015552
OS [37] B-A-B	600	0.05	80	0.021446	0.014528	0.360014	0.025920	0.001555
Coll.[24]p=1	1000	0.05	80	0.014	0.015	0.36	0.0259	0.0016
Coll.[24]p=0.0000339263	1000	0.05	80	0.0039	0.0017	0.36	0.0259	0.0016
Coll.[24]p=1	2000	0.05	80	0.27	0.20	0.36	0.0259	0.0016
Coll.[24]p=0.0000010587	2000	0.05	80	0.067	0.025	0.36	0.0259	0.0016
Coll. [17]	2000	0.05	80	0.01064	0.01485	0.36001	0.02592	0.00156
PG [29]	600	0.05	80	0.010249	0.014128	0.360013	0.02592	0.0015552
FDM. [34]	600	0.05	80	0.0436	0.0309	0.36001	0.02592	0.00156
Lum.Gal. [35]	600	0.05	80	0.013	0.007	0.36000	0.02592	0.00156
FIFDM[36]	600	0.05	80	0.04360	0.03095	0.36001	0.02592	0.00156
LS[26] $0\le x\le20$	200	0.05	80	0.22	0.16	0.3593	0.0259	0.00155
RBFC [30] MQ	200	0.5	80	0.03566	0.01918	0.359971	0.025921	0.001555
RBFC [30] G	200	0.5	80	0.00401	0.00151	0.360016	0.025921	0.001555
RBFC [30] IQ	200	0.5	80	0.06510	0.07056	0.359976	0.025920	0.001555
RBFC [30] IMQ	200	0.5	80	0.18717	0.16896	0.360385	0.025920	0.001555
Analytic						0.360000	0.025920	0.001555

Table 5: Single solitary wave: $c = 0.01, \mu = 1,\ 0 \le x \le 30$.

Method	N	Δt	t	$L_2\times10^3$	$L_\infty\times10^3$	I_1	I_2	I_3
DQM(Pres.)	190	0.05	0	0.000000	0.000000	0.119995	0.002880	0.000058
			10	0.003775	0.004929	0.119990	0.002880	0.000058
			20	0.003412	0.004460	0.119991	0.002880	0.000058
			30	0.003097	0.004036	0.119992	0.002880	0.000058
			40	0.002796	0.003652	0.119992	0.002880	0.000058
			50	0.002534	0.003304	0.119993	0.002880	0.000058
			60	0.002297	0.002990	0.119994	0.002880	0.000058
			70	0.002076	0.002705	0.119994	0.002880	0.000058
			80	0.001889	0.002448	0.119995	0.002880	0.000058
Gal. [13]	600	0.05	0	0.001	0.005	0.11999	0.00288	0.000058
			10	0.039	0.030	0.12009	0.00288	0.000058
			20	0.083	0.061	0.12021	0.00289	0.000058
			30	0.130	0.091	0.12033	0.00289	0.000058
			40	0.174	0.119	0.12045	0.00290	0.000058
			50	0.215	0.144	0.12056	0.00290	0.000058
			60	0.254	0.167	0.12067	0.00291	0.000058
			70	0.292	0.188	0.12078	0.00291	0.000058
			80	0.330	0.206	0.12088	0.00291	0.000059
MOL. [32]	600	0.05	80	0.005536	0.002853	0.120000	0.00287993	0.0000576
FDM. [34]	600	0.05	80	0.0054	0.0036	0.12000	0.00288	0.00006
Lum.Gal.[35]	600	0.05	80	0.003	0.002	0.12000	0.00288	0.000058
Gal. [16]	600	0.05	80	0.001757	0.002448	0.12000	0.00288	0.000058
LS[26] 0≤x≤20	200	0.1	80	0.0177	0.0127	0.1200	0.00288	0.000058
Analytic						0.120000	0.002880	0.000058

Table 6: The three invariants for boundary-forcing: $U_0 = 1, U_0 = 2, U_0 = 3$

	$U_0 = 1$			$U_0 = 2$			$U_0 = 3$		
t	I_1	I_2	I_3	I_1	I_2	I_3	I_1	I_2	I_3
10	5.15014	5.58966	5.56139	20.00252	48.03358	103.8709	45.7195	173.2326	580.634
20	10.04755	12.06387	13.03831	40.77405	104.72660	236.4028	90.0124	349.9052	1185.730
30	13.67962	17.79670	19.47428	56.76358	149.82370	333.5779	130.0428	518.6323	1736.460
40	14.02851	17.66647	19.53212	58.17610	148.63920	334.3503	132.5307	515.4232	1742.136
50	14.12945	17.64571	19.53544	58.25787	148.63780	334.3793	132.5353	515.4432	1742.433
60	14.19259	17.64000	19.53659	58.26126	148.63720	334.3772	132.5386	515.4442	1742.473
70	14.22699	17.63861	19.53675	58.26175	148.63520	334.3619	132.5415	515.4479	1742.531
80	14.24390	17.63826	19.53655	58.26214	148.63730	334.3849	132.5442	515.4539	1742.634
90	14.25181	17.63812	19.53623	58.26252	148.63680	334.3820	132.5466	515.4496	1742.560
100	14.25541	17.63806	19.53592	58.26282	148.63710	334.3831	132.5488	515.4499	1742.571
110	14.25705	17.63800	19.53567	58.26313	148.63840	334.3971	132.5506	515.4500	1742.581
120	14.25781	17.63799	19.53554	58.26342	148.63780	334.3920	132.5524	515.4542	1742.626
130	14.25816	17.63801	19.53554	58.26368	148.63700	334.3807	132.5538	515.4551	1742.646
140	14.25834	17.63804	19.53564	58.26393	148.63750	334.3889	132.5552	515.4460	1742.505
150	14.25843	17.63810	19.53587	58.26418	148.63960	334.4076	132.5564	515.4534	1742.625

Table 7: The three invariants, location and amplitude of the leading undulation: $\Delta t = 0.2$, $h = 0.2$.

d	t	I_1	I_2	I_3	x	U
1	0	2.009999	0.196555	0.019350	-	-
	200	3.010007	0.329909	0.034358	9.6	0.17748
	400	4.010017	0.463265	0.049367	21.6	0.18114
	600	5.010021	0.596621	0.064375	25.6	0.17485
	800	6.009983	0.729979	0.079384	41.6	0.17976
2	0	2.010000	0.191278	0.018600	-	-
	200	3.010007	0.324627	0.033606	9.4	0.17607
	400	4.010014	0.457983	0.048615	21.4	0.18177
	600	5.010022	0.591340	0.063624	25.4	0.17261
	800	6.010003	0.724696	0.078633	41.2	0.18153
5	0	2.010080	0.176127	0.016352	-	-
	200	3.010088	0.309468	0.031355	8.8	0.16054
	400	4.010093	0.442822	0.046363	20.4	0.17936
	600	5.010102	0.576179	0.061372	32.6	0.18013
	800	6.010105	0.709535	0.076381	44.8	0.18280
10	0	2.018873	0.152827	0.012865	-	-
	200	3.018983	0.286180	0.027867	7.8	0.09274
	400	4.018984	0.419525	0.042872	19.2	0.16704
	600	5.018990	0.552880	0.057880	31.0	0.17951
	800	6.018996	0.686235	0.072889	43.2	0.18074

Biography

Ali Başhan is currently working as an Associate Professor in the Department of Mathematics at the Bursa Technical University, Bursa, Türkiye. He obtained his Ph.D. degree in the field of Applied Mathematics from Inonu University, Malatya, Türkiye. He has published over 30 articles peer-reviewed journals. The main field of his activity includes development of numerical algorithms for nonlinear partial differential equations.